Condensed Matter Physics, 2001, Vol. 4, No. 3(27), pp. 523–552

CONDENSED MATTER PHYSICS

Thermodynamics and dielectric properties of KH_2PO_4, RbH_2PO_4, KH_2AsO_4, RbH_2AsO_4 ferroelectrics

R.R.Levitskii, B.M.Lisnii, O.R.Baran

Institute for Condensed Matter Physics
of the National Academy of Sciences of Ukraine,
1 Svientsitskii Str., 79011 Lviv, Ukraine

Received May 28, 2001

Within the proton ordering model with taking into account the short-range and long-range interactions as well as tunnelling effects, in the framework of the cluster approximation, we study the thermodynamic and static dielectric properties of the KH_2PO_4 type ferroelectrics. Theoretical results are compared with the corresponding experimental data and with the results of theoretical calculations of other sources. We show that under the proper choice of the theory parameters, a very good quantitative description of the available experimental data is obtained for the temperature dependence of spontaneous polarization, specific heat, longitudinal and transverse static dielectric permittivities, as well for the Curie-Weiss temperature and constant.

Suitability of the model for the description of experimental data for the crystals KH_2PO_4, RbH_2PO_4, KH_2AsO_4, RbH_2AsO_4 without taking into account striction, fluctuations, and other effects is discussed.

Key words: *cluster approximation, KDP, tunnelling, phase transition, dielectric permittivity, Curie-Weiss temperature, Curie-Weiss constant*

PACS: *77.22.Ch, 77.80.Bh, 77.84.Fa*

1. Introduction

Since the discovery of the ferroelectric properties of the KH_2PO_4 (KDP), this and isomorphic crystals attract a considerable interest of both theorists and experimentalists, mainly because of their relatively simple structure and special properties related to the system of hydrogen bonds. A noticeable peculiarity in the development of the physics of these crystals is a strong connection between theory and experiment which enabled a remarkable progress in understanding the microscopic properties of the crystals and in developing their theoretical models.

A proton ordering model for the theoretical description of the KDP type crystals

was proposed by Blinc [1]. He considered a model based on the assumptions that protons move on hydrogen bonds in double well potential, and that the tunnelling effects are present. From these assumptions, de Gennes [2] proposed a pseudospin model that takes into account a quantum motion of protons on hydrogen bonds. This model has been later developed in a series of publications. Tokunaga and Matsubara [3] obtained the basic Hamiltonian from rather general principles, whereas Kobayashi [4] developed an adequate dynamic description of the phase transition. At the same time, Blinc and Svetina [5], taking into account the proton tunnelling and, partially, the proton-lattice interaction, developed the cluster approximation for the free energy in the short-range interactions, with taking into account the long-range interactions within the mean field approximation. The authors reduced its calculation to numerical solution of a system of transcendent equations. Studies of the influence of the tunnelling integral and the other model parameters on polarization, specific heat, transition entropy, as well as on the order and temperature of the phase transition have shown that taking tunnelling into account improves an agreement between the theory and the experiment, as compared to a classical version of the model. Later [6], possible types of proton ordering were found, conditions for their realization were formulated, and a key role of the long-range interactions in establishing an antipolarized state in the $ND_4D_2PO_4$ type antiferroelectrics was shown.

Vaks and Zinenko [7] attempted to analytically calculate the free energy obtained in the cluster approximation by Blinc and Svetina, restricting themselves to the first order expansion of eigenvalues in small parameters and making some approximations when solving the transcendent equations for the cluster parameters. However, such a method yielded a too large error (even near the transition temperature it was about 10% [8]). Therefore, a poor agreement of the theoretical results with experimental data followed. Let us note that an important point in this paper is to discuss an unphysical behaviour of the tunnelling model at low temperatures [5]. Later in the paper [9] all crystals of the KDP type were studied using the previous results [7].

Especially we would like to point to the paper by Vaks et al [8], where a numerical investigation of the dependences of the thermodynamic characteristics of the KDP family ferroelectrics on the model parameters was performed within the cluster approximation. However, even though this paper was a certain summing up of the active studies of the proton model initiated by Blinc and Svetina, it does not give a comprehensive answer regarding all the resources of the model in describing the experimental data for the KDP type crystals. The same applies to the paper [10], where the parameters obtained in [8] were corrected in order to improve a description of the experimental data for polarization in these crystals.

Expansion of the pseudospin model for the theoretical investigation of the transverse dielectric properties of the KDP type crystals was proposed by Havlin et al. in [11–14]. It was shown that the mean field approximation does not provide a good agreement of the theoretically calculated transverse permittivity with the experimental one at temperatures below the transition point [11], whereas a cluster approximation for the classical version of the pseudospin model (without tunnelling)

yields fair results for describing of the dielectric properties of deuterated KD_2PO_4 type crystals [13] but is not quite suitable for undeuterated KH_2PO_4 type crystals [12] where the tunnelling effects should be taken into account. An attempt to take into account the tunnelling within the cluster approximation was made in [14], where the transverse dielectric permittivity was calculated numerically from the self-consistency equations; however, the description of the experimental data was not satisfactory.

We should separately mention the papers [15–19] where it was shown that thermodynamic and dynamics properties of the KH_2PO_4 (KDP), RbH_2PO_4 (RDP), KH_2AsO_4 (KDA), RbH_2AsO_4 (RDA) crystals can be satisfactorily described within a classical version of the proton model, which corresponds to deuterated crystals.

Hence, it is generally accepted that the phase transition in the KDP type crystals is strongly related to proton ordering in double well potentials. Until the middle 80-ies, the proton model was an established basis for a description of the phase transition in the KDP. Doubts in its validity were raised by Raman scattering experiments in these crystals, because the soft mode coupled to proton motion was not revealed (see [20–22]). In 1984 Tokunaga [23] proposed a new model of the phase transitions in the KDP crystals, according to which the ferroelectric transition results from ordering of the H_2PO_4 dipoles. However, the elaboration level of this model is very low. Thus, it is still unclear whether it permits to quantitatively describe the peculiarities of static and dynamic characteristics of the crystals. Here it should be noted that in practical realization of such a model some complications arise, related to breaking the "ice rule" in the ordered phase (see [24]). The data of [25] also do not support the idea about ordering of the H_2PO_4 groups but rather give evidence for the proton ordering. Therefore, a model other than the proton model, which would agree with the light scattering experiments, pressure effects, and some other experimental facts, does not exist at the moment.

Our goal is a theoretical study and comparison with the experimental data of thermodynamic and static dielectric properties of undeuterated KDP type crystals within the proton ordering model with tunnelling and cluster approximation for the free energy. For this purpose, we use the theoretical results of our previous work [26] where the static dielectric susceptibility tensor was obtained theoretically for the first time, as well as the numerical method of an unambiguous setting of optimal values of the model parameters proposed therein.

2. The Hamiltonian. Four-particle cluster approximation

Let us consider a system of protons in KH_2PO_4 type ferroelectrics, moving on the O–H...O-bonds that link PO_4 tetrahedra. The primitive cell of Bravais lattice consists of two neighbouring tetrahedra PO_4 along with four hydrogen bonds attached to one of them. The bonds attached to the other tetrahedron belong to the four nearest structural elements surrounding it (see figure 1). An effective Hamiltonian of proton subsystem of the KDP type ferroelectrics that takes into account short-range and long-range interactions as well as the effects of proton tunnelling

has the following form [3,5,6]:

$$\hat{H} = -2\Omega \sum_{\boldsymbol{n},f} \hat{S}_f^x(\boldsymbol{n}) - \frac{1}{2} \sum_{\boldsymbol{n}_1\boldsymbol{n}_2} \sum_{f_1 f_2} J_{f_1 f_2}(\boldsymbol{n}_1, \boldsymbol{n}_1) \hat{S}_{f_1}^z(\boldsymbol{n}_1) \hat{S}_{f_2}^z(\boldsymbol{n}_2)$$
$$+ \sum_{\substack{\boldsymbol{n}_1,\boldsymbol{n}_2 \\ \boldsymbol{n}_3,\boldsymbol{n}_4}} \Big\{ \frac{1}{2} \sum_{f_1,f_2} V_{f_1 f_2} \hat{S}_{f_1}^z(\boldsymbol{n}_1) \hat{S}_{f_2}^z(\boldsymbol{n}_2) + \Phi \hat{S}_1^z(\boldsymbol{n}_1) \hat{S}_2^z(\boldsymbol{n}_2) \hat{S}_3^z(\boldsymbol{n}_3) \hat{S}_4^z(\boldsymbol{n}_4) \Big\}$$
$$\times \{ \delta_{\boldsymbol{n}_1,\boldsymbol{n}_2} \delta_{\boldsymbol{n}_1,\boldsymbol{n}_3} \delta_{\boldsymbol{n}_1,\boldsymbol{n}_4} + \delta_{\boldsymbol{n}_1+\boldsymbol{r}_2,\boldsymbol{n}_2} \delta_{\boldsymbol{n}_1+\boldsymbol{r}_3,\boldsymbol{n}_3} \delta_{\boldsymbol{n}_1+\boldsymbol{r}_4,\boldsymbol{n}_4} \}. \qquad (2.1)$$

Here the first term describes proton tunnelling on the O–H...O-bonds; the second one corresponds to the long-range interactions between protons including an effective lattice mediated interaction as well; the third term is the short-range configurational correlations between protons around a PO_4 group; $\hat{S}_f^\alpha(\boldsymbol{n})$ is the α-component ($\alpha = x, z$) of the pseudospin operator $\hat{\boldsymbol{S}}_f(\boldsymbol{n})$ which characterises the state of a proton on the f-th bond ($f = 1, 2, 3, 4$) in the $\boldsymbol{n}$-th cell: the eigenvalues of the operator $\hat{S}_f^z(\boldsymbol{n}) = \pm\frac{1}{2}$ correspond to two equilibrium proton sites on a bond; $\boldsymbol{r}_f$ is radius-vector of a relative position of the hydrogen bond in a primitive cell.

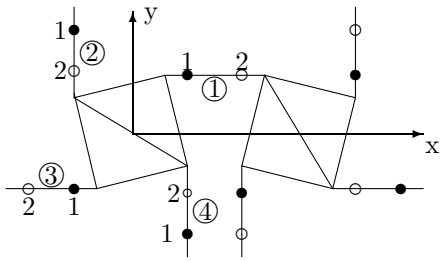

①, ②, ③, ④ numerate hydrogen bonds; 1, 2 are equilibrium proton sites on a bond. One of possible ferroelectric proton configurations is shown.

Figure 1. Primitive cell of the KDP type crystal.

Within the four-particle cluster approximation for the short-range interactions and the mean field approximation for the long-range interactions, the free energy of a proton subsystem of the KH_2PO_4 type ferroelectrics per primitive cell reads [5,6,26]:

$$f = -2\beta^{-1} \left(\ln Z_4 - 2 \ln Z_1^f \right) + \frac{1}{2} \nu_z P^2, \qquad (2.2)$$

where $\beta = (k_{\rm B}T)^{-1}$, $k_{\rm B}$ is the Boltzmann constant; T is the absolute temperature; $P = \langle 2\hat{S}_f^z(\boldsymbol{n}) \rangle$ is the parameter of hydrogen ordering; ν_z is constant of the long-range interactions (dipole-dipole and lattice mediated); $Z_4 = \mathrm{Sp}\, \mathrm{e}^{-\beta \hat{H}_4}$, $Z_1^f = \mathrm{Sp}\, \mathrm{e}^{-\beta \hat{H}_1^f}$ are four-particle and single particle partition functions; the four-particle cluster Hamiltonian $\hat{H}_4$ and single-particle Hamiltonians $\hat{H}_1^f$ read [26]

$$\hat{H}_4 = 2\Gamma \sum_{f=1}^{4} \hat{S}_f^x + V(\hat{S}_1^z \hat{S}_2^z + \hat{S}_2^z \hat{S}_3^z + \hat{S}_3^z \hat{S}_4^z + \hat{S}_4^z \hat{S}_1^z)$$
$$+ \; U(\hat{S}_1^z \hat{S}_3^z + \hat{S}_2^z \hat{S}_4^z) + \Phi \hat{S}_1^z \hat{S}_2^z \hat{S}_3^z \hat{S}_4^z + C \sum_{f=1}^{4} \hat{S}_f^z \,, \qquad (2.3)$$

$$\hat{H}_1^f = 2(2\Gamma + \Omega)\hat{S}_f^x + 2(C + \frac{1}{4}\nu_z P)\hat{S}_f^z\ , \quad f = \overline{1,4},$$

where the constant of interactions is related to the Slater–Takagi energies as [3,5,6]:

$$V = V_{12} = V_{23} = V_{34} = V_{41} = -\frac{1}{2}w_1,$$

$$U = V_{13} = V_{24} = -\varepsilon + \frac{1}{2}w_1, \quad \Phi = 4\varepsilon - 8w + 2w_1.$$

The fields Γ and C are

$$\Gamma = -\Omega + \frac{\eta}{4}, \quad C = \Delta - \frac{1}{2}\nu_z P.$$

The cluster parameters η and Δ are to be found from the free energy minimum condition [5–7]

$$\frac{\partial f}{\partial \eta} = \frac{\partial f}{\partial \Delta} = 0,$$

which for the first order of cluster approximation is nothing but the condition of self-consistency [5,6,26]: the pseudospin mean values calculated with the cluster Hamiltonian and with the single-particle Hamiltonian

$$\begin{aligned} \langle 2\hat{S}_f^x(\boldsymbol{n})\rangle_{(4)} &= \langle 2\hat{S}_f^x(\boldsymbol{n})\rangle_{(1)} \equiv X, \\ \langle 2\hat{S}_f^z(\boldsymbol{n})\rangle_{(4)} &= \langle 2\hat{S}_f^z(\boldsymbol{n})\rangle_{(1)} \equiv P \end{aligned} \tag{2.4}$$

should coincide.

For subsequent calculations we need to find the eigenvalues of the Hamiltonians (2.3). For the single-particle Hamiltonian this task can be easily soft by rotation of quasispin operators

$$Z_1 = 2\mathrm{ch}(\beta\sqrt{K}), \quad K = (C + \frac{1}{4}\nu_z P)^2 + (2\Gamma + \Omega)^2. \tag{2.5}$$

To find the eigenvalues of the four-particle Hamiltonian is a more complicated task. We should, first, perform a unitary transformation, taking into account the fact that its symmetry group is isomorphic to the point group D_4 in the ferroelectric phase and to D_{4h} in the paraelectric phase. After that, subtracting a constant, we obtain a matrix of the Hamiltonian $\hat{H}_4$ in the following form:

$$H_4 = B_1 \oplus B_2 \oplus B_2 \oplus B_3 \oplus B_4,$$

$$B_1 = \begin{pmatrix} -2C & 0 & 0 & 2\Gamma & 0 & 0 \\ 0 & 2C & 0 & 0 & 2\Gamma & 0 \\ 0 & 0 & \varepsilon & 2\Gamma & 2\Gamma & 0 \\ 2\Gamma & 0 & 2\Gamma & w - C & 0 & \sqrt{2}\Gamma \\ 0 & 2\Gamma & 2\Gamma & 0 & w + C & \sqrt{2}\Gamma \\ 0 & 0 & 0 & \sqrt{2}\Gamma & \sqrt{2}\Gamma & w_1 \end{pmatrix},$$

$$B_2 = \begin{pmatrix} \varepsilon & \sqrt{2}\Gamma & \sqrt{2}\Gamma \\ \sqrt{2}\Gamma & w-C & 0 \\ \sqrt{2}\Gamma & 0 & w+C \end{pmatrix}, \quad B_3 = \varepsilon,$$

$$B_4 = \begin{pmatrix} w-C & 0 & \sqrt{2}\Gamma \\ 0 & w+C & \sqrt{2}\Gamma \\ \sqrt{2}\Gamma & \sqrt{2}\Gamma & w_1 \end{pmatrix} \tag{2.6}$$

in the ferroelectric phase and

$$H_4^p = B_1^p \oplus B_2^p \oplus B_3^p \oplus B_4^p \oplus B_3^p \oplus B_4^p \oplus B_5^p \oplus B_6^p \oplus B_4^p,$$

$$B_1^p = \begin{pmatrix} 0 & 0 & 2\Gamma & 0 \\ 0 & \varepsilon & 2\sqrt{2}\Gamma & 0 \\ 2\Gamma & 2\sqrt{2}\Gamma & w & 2\Gamma \\ 0 & 0 & 2\Gamma & w_1 \end{pmatrix},$$

$$B_2^p = \begin{pmatrix} 0 & 2\Gamma \\ 2\Gamma & w \end{pmatrix}, \quad B_3^p = \begin{pmatrix} \varepsilon & 2\Gamma \\ 2\Gamma & w \end{pmatrix},$$

$$B_4^p = w, \quad B_5^p = \varepsilon, \quad B_6^p = \begin{pmatrix} w_1 & 2\Gamma \\ 2\Gamma & w \end{pmatrix} \tag{2.7}$$

in the high-temperature phase ($C = 0$). Matrices (2.6) coincide with their analogs given in [7,27] and are equivalent to the matrices found in [5] (coincide with those after a unitary transformation). The eigenvalues of the H_4 and H_4^p matrices are obtained in the following form

$$\begin{aligned} &E_i, \quad i = \overline{1,6} - \text{roots of the equation} \\ &\quad E^6 + E^5 k_5 + E^4 k_4 + E^3 k_3 + E^2 k_2 + E k_1 + k_0 = 0; \\ &E_i = E_{i+3}, \quad i = \overline{7,9} - \text{roots of the equation} \\ &\quad E^3 + E^2 l_2 + E l_1 + l_0 = 0; \\ &E_{13} = \varepsilon; \quad E_i,\ i = 14,15,16 - \text{roots of the equation} \\ &\quad E^3 + E^2 m_2 + E m_1 + m_0 = 0 \end{aligned} \tag{2.8}$$

in the ferroelectric phase and

$$\begin{aligned} &E_{pi}, \quad i = \overline{1,4} - \text{roots of the equation} \\ &\quad E^4 + E^3(-\varepsilon - w - w_1) + E^2(\varepsilon w + \varepsilon w_1 + w w_1 - 16\Gamma^2) \\ &\quad + E((8\varepsilon + 12 w_1)\Gamma^2 - \varepsilon w w_1) - 4\varepsilon w_1 \Gamma^2 = 0; \\ &E_{p5,6} = \frac{1}{2}(w \pm \sqrt{w^2 + 16\Gamma^2}), \\ &E_{p7,8} = \frac{1}{2}(w + \varepsilon \pm \sqrt{(w-\varepsilon)^2 + 16\Gamma^2}), \\ &E_{p10,11} = \frac{1}{2}(w + \varepsilon \pm \sqrt{(w-\varepsilon)^2 + 16\Gamma^2}), \\ &E_{p9} = E_{p12} = E_{p16} = w, \qquad E_{p13} = \varepsilon, \\ &E_{p14,15} = \frac{1}{2}(w + w_1 \pm \sqrt{(w-w_1)^2 + 16\Gamma^2}) \end{aligned} \tag{2.9}$$

in the high-temperature phase. Here we used the notations:

$$
\begin{aligned}
k_0 &= -4C^2\varepsilon w_1 w^2 + 4C^4 w_1\varepsilon + 16\Gamma^4 w_1\varepsilon + 16\Gamma^2 C^2(w\varepsilon + 2ww_1 - \varepsilon w_1),\\
k_1 &= 4C^2(w^2(w_1+\varepsilon) + 2w_1 w\varepsilon) - 16\Gamma^2 C^2(3w + w_1) - 4C^4(\varepsilon + w_1)\\
&\quad -16\Gamma^4(3w_1 + 2\varepsilon) + 8\Gamma^2 w_1 w\varepsilon,\\
k_2 &= w^2 w_1\varepsilon - C^2(8w(w_1+\varepsilon) + 5w_1\varepsilon + 4w^2) + 32\Gamma^2 C^2 + 4C^4\\
&\quad -4\Gamma^2(2w_1\varepsilon + 3w\varepsilon + 4w_1 w) + 64\Gamma^4,\\
k_3 &= -w^2(w_1+\varepsilon) - 2w_1 w\varepsilon + C^2(8w + 5w_1 + 5\varepsilon)\\
&\quad +4\Gamma^2(3\varepsilon + 4w_1 + 5w),\\
k_4 &= 2w(w_1+\varepsilon) + w^2 + w_1\varepsilon - 5C^2 - 20\Gamma^2,\\
k_5 &= -2w - w_1 - \varepsilon,\\
l_0 &= -w^2\varepsilon + C^2\varepsilon + 4\Gamma^2 w, \quad l_1 = w^2 + 2w\varepsilon - C^2 - 4\Gamma^2,\\
l_2 &= -2w - \varepsilon, \quad m_0 = -w^2 w_1 + C^2 w_1 + 4\Gamma^2 w,\\
m_1 &= w^2 + 2ww_1 - C^2 - 4\Gamma^2, \quad m_2 = -w_1 - 2w.
\end{aligned}
$$

Hence, in this section we presented the Hamiltonian of the proton subsystem of the KH_2PO_4 type ferroelectrics and the free energy, obtained in the first order of the cluster approximation for the short-range interactions and in the mean field approximation for the long-range interactions. We show that the calculation of the free energy in this approximation is reduced to the calculation of eigenvalues of the quasidiagonal matrices (2.6) and (2.7) or to the solution of algebraic equations (2.8) and (2.9). This fact will be used in numerical calculations.

3. Thermodynamics of the KDP type ferroelectrics

Let us consider now thermodynamic characteristics of the system. The free energy of the proton subsystem of the KH_2PO_4 type ferroelectrics (2.2), with taking into account (2.5) and (2.8), can be written as

$$f = -2\beta^{-1}(\ln Z_4 - 2\ln Z_1) + \frac{1}{2}\nu_z P^2, \quad Z_4 = \sum_{i=1}^{16}\exp(-\beta E_i). \tag{3.1}$$

Differentiating the free energy, we obtain the entropy of proton subsystem

$$S = -\frac{1}{T}f + \frac{1}{2T}\nu_z P^2 + \frac{2}{T}\frac{1}{Z_4}\sum_{i=1}^{16}\exp(-\beta E_i)E_i + \frac{4}{T}\sqrt{K}\tanh(\beta\sqrt{K}). \tag{3.2}$$

Unknown fields Γ and C, entering these expressions and containing the cluster fields Δ and η, as well as the proton ordering parameter P, can be found from the following system of equations for X and P, obtained from the self-consistency condition and after the change of variables reduced to

$$\begin{cases} P = \frac{1}{2Z_4}\sum\limits_{i=1}^{16}\exp(-\beta E_i)E_{iC}, \\ X = \frac{1}{4Z_4}\sum\limits_{i=1}^{16}\exp(-\beta E_i)E_{i\Gamma}, \end{cases} \tag{3.3}$$

where

$$C = \frac{P}{2\beta Q}\ln\frac{1-Q}{1+Q} - \frac{1}{4}\nu_z P,$$
$$\Gamma = \frac{X}{4\beta Q}\ln\frac{1-Q}{1+Q} - \frac{\Omega}{2},$$
$$Q = \sqrt{P^2+X^2}. \tag{3.4}$$

Here we used the following notations

$$E_{iC} = -\frac{E_i^4 k_{4C} + E_i^3 k_{3C} + E_i^2 k_{2C} + E_i k_{1C} + k_{0C}}{6E_i^5 + 5E_i^4 k_5 + 4E_i^3 k_4 + 3E_i^2 k_3 + 2E_i k_2 + k_1},$$
$$k_{0C} = -8Cw^2 w_1\varepsilon + 16C^3 w_1\varepsilon + 32\Gamma^2 C(w\varepsilon + 2w_1 w - \varepsilon w_1),$$
$$k_{1C} = 8C(w^2(w_1+\varepsilon)+2w_1 w\varepsilon) - 32\Gamma^2 C(3w+w_1) - 16C^3(w_1+\varepsilon),$$
$$k_{2C} = -2C(8w(w_1+\varepsilon) + 5w_1\varepsilon + 4w^2) + 64\Gamma^2 C + 16C^3,$$
$$k_{3C} = 2C(8w + 5w_1 + 5\varepsilon), \quad k_{4C} = -10C, \quad i = \overline{1,6}\ ;$$
$$E_{iC} = \frac{2C(E_i - \varepsilon)}{3E_i^2 + 2E_i l_2 + l_1}, \quad i = \overline{7,12}; \quad E_{13C} = 0;$$
$$E_{iC} = \frac{2C(E_i - w_1)}{3E_i^2 + 2E_i m_2 + m_1}, \qquad i = 14,15,16;$$
$$E_{i\Gamma} = -\frac{E_i^4 k_{4\Gamma} + E_i^3 k_{3\Gamma} + E_i^2 k_{2\Gamma} + E_i k_{1\Gamma} + k_{0\Gamma}}{6E_i^5 + 5E_i^4 k_5 + 4E_i^3 k_4 + 3E_i^2 k_3 + 2E_i k_2 + k_1},$$
$$k_{0\Gamma} = -64\Gamma^3 w_1\varepsilon + 32\Gamma C^2(w\varepsilon + 2w_1 w - \varepsilon w_1),$$
$$k_{1\Gamma} = -32\Gamma C^2(3w + w_1) - 64\Gamma^3(3w_1 + 2\varepsilon) + 16\Gamma w_1 w\varepsilon,$$
$$k_{2\Gamma} = -8\Gamma(2w_1\varepsilon + 3w\varepsilon + 4w_1 w) + 64\Gamma C^2 + 256\Gamma^3,$$
$$k_{3\Gamma} = 8\Gamma(3\varepsilon + 4w_1 + 5w), \quad k_{4\Gamma} = -40\Gamma, \quad i = \overline{1,6}\ ;$$
$$E_{i\Gamma} = \frac{8\Gamma(E_i - w)}{3E_i^2 + 2E_i l_2 + l_1}, \quad i = \overline{7,12}; \quad E_{13\Gamma} = 0;$$
$$E_{i\Gamma} = \frac{8\Gamma(E_i - w)}{3E_i^2 + 2E_i m_2 + m_1}, \quad i = 14,15,16.$$

The derived expression for the specific heat is too cumbersome to be presented here. In numerical calculations it was obtained by numerical differentiation of entropy with respect to temperature.

It is known [28] that ferroelectric polarization of a KH_2PO_4 type crystal is related to the proton ordering parameter P as

$$\mathcal{P} = \sum_{f=1}^{4}\frac{\mu_z}{v}\langle\hat{S}_f^z(\mathbf{n})\rangle = 2\frac{\mu_z}{v}P, \tag{3.5}$$

where v is the primitive cell volume, and μ_z is an effective dipole moment along the ferroelectric axis z per hydrogen bond.

The condition of continuity of the free energy at the first order phase transition and the above system of equations (3.3) yield the system of equations for the transition temperature $T_{\rm c}$:

$$\begin{cases} f(P,X,T_{\rm c}) = f(0,X,T_{\rm c}), \\ P = \frac{1}{2Z_4}\sum\limits_{i=1}^{16}\exp(-\beta_{\rm c}E_i)E_{iC}, \\ X = \frac{1}{4Z_4}\sum\limits_{i=1}^{16}\exp(-\beta_{\rm c}E_i)E_{i\Gamma}, \end{cases} \tag{3.6}$$

where all quantities are taken at $T = T_{\rm c}$.

Hence, in this section we obtain the major thermodynamic characteristics of the KH_2PO_4 type ferroelectrics. To calculate these characteristics, one has to solve the system of two equations with unknown X and P and simultaneously to find the eigenvalues of the four-particle cluster Hamiltonian using one of the methods shown in the previous section.

4. Static dielectric permittivity

In this section we shall study the static dielectric properties of a proton subsystem of a ferroelectric KH_2PO_4 type crystals. Details of the calculations are given in [26]; in this paper we shall only consider the main ideas of the calculations and present the final results. Hence, let us place the crystal in a weak constant electric field $\mathbf{E} = (E_x, E_y, E_z)$. Hamiltonian of the proton subsystem then reads

$$\hat{H}_{\mathbf{E}} = \hat{H} + \hat{V},$$

where $\hat{V}$ is the interaction of protons with the electric field $\mathbf{E}$. Here $\hat{H}$ is the known Hamiltonian (2.1), whereas $\hat{V}$ describes interaction of protons with the electric field:

$$\hat{V} = -\sum_{\mathbf{n},f}(\boldsymbol{\mu}_f\mathbf{E})\hat{S}_f^z(\mathbf{n}).$$

Here $\boldsymbol{\mu}_f = (\mu_f^x, \mu_f^y, \mu_f^z)$ is the effective dipole moment of the f-th bond of a primitive cell. Its components obey the following relations

$$\begin{aligned} &-\mu_1^x = \mu_3^x = \mu_x, \quad -\mu_4^y = \mu_2^y = \mu_y, \\ &\mu_1^y = \mu_3^y = \mu_2^x = \mu_4^x = 0, \quad \mu_1^z = \mu_2^z = \mu_3^z = \mu_4^z = \mu_z, \end{aligned}$$

which result from the symmetry of the system of hydrogen bonds and from the character of proton ordering in the electric field [11–14]. Taking into account the structure of the mean values of pseudospins in a macroscopic electric field

$$\langle 2\hat{S}_f^z(\mathbf{n})\rangle = P + P_f, \quad \langle 2\hat{S}_f^x(\mathbf{n})\rangle = X + X_f,$$

$$P_f|_{\mathbf{E}=0} = 0, \quad X_f|_{\mathbf{E}=0} = 0, \quad f = \overline{1,4},$$

we obtain the following cluster and single-particle Hamiltonians:

$$\hat{H}_{4E} = \hat{H}_4 + \sum_{f=1}^{4} \eta_f \hat{S}_f^x + \sum_{f=1}^{4} C_f \hat{S}_f^z,$$

$$\hat{H}_{1E}^{(f)} = 2(2\Gamma{+}\Omega{+}\eta_f)\hat{S}_f^x{+}2\left(C{+}\frac{1}{4}\nu_z P{+}C_f{+}\frac{1}{4}\sum_{f_1} J_{ff_1}(0)P_{f_1}{+}\frac{1}{2}\boldsymbol{\mu}_f\mathbf{E}\right)\hat{S}_f^z,$$

where $\hat{H}_4$ is the known Hamiltonian (2.3),

$$C_f = \Delta_f - \frac{1}{2}\sum_{f_1} J_{ff_1}P_{f_1} - \boldsymbol{\mu}_f\mathbf{E},$$

whereas η_f and Δ_f are field induced cluster fields; hence

$$\eta_f = \Delta_f = 0 \quad \text{at} \quad \mathbf{E} = 0.$$

We suppose the polarization $\mathcal{P} = (\mathcal{P}_x, \mathcal{P}_y, \mathcal{P}_z)$ of a crystal is related to the mean values of the pseudospins as [11–14,26]:

$$\mathcal{P}_x = \frac{\mu_x}{2v}(P_3 - P_1), \quad \mathcal{P}_y = \frac{\mu_y}{2v}(P_2 - P_4), \quad \mathcal{P}_z = \frac{\mu_z}{2v}(4P + \sum_{f=1}^{4} P_f).$$

Hence, to find tensor of static dielectric susceptibility

$$\chi_{\alpha\beta} = \left.\frac{\mathrm{d}\mathcal{P}_\alpha}{\mathrm{d}E_\beta}\right|_{\mathbf{E}=0} \qquad (\alpha, \beta = x, y, z),$$

we need to find the derivatives $P_{f\alpha} = \left.\frac{\mathrm{d}P_f}{\mathrm{d}E_\alpha}\right|_{\mathbf{E}=0}$, $\alpha = x, y, z$, $f = \overline{1,4}$. According to [26], from the self-consistency condition (2.4) we obtain a system of equation for cluster fields η_f and Δ_f which we reduce to the form (3.3), where the fields are explicitly expressed via the unknown X_f and P_f. The obtained system of equations is differentiated with respect to the field components E_α; then the limit $\mathbf{E} \to 0$ is performed. We get the following linear system of equations for the sought derivatives $P_{f\alpha}$:

$$\begin{cases} P_{f\alpha} = \sum\limits_{f_1=1}^{4} R_{ff_1} C_{f_1\alpha} + \sum\limits_{f_1=1}^{4} M_{ff_1}\eta_{f_1\alpha}, \\ X_{f\alpha} = \sum\limits_{f_1=1}^{4} M_{ff_1} C_{f_1\alpha} + \sum\limits_{f_1=1}^{4} N_{ff_1}\eta_{f_1\alpha}, \end{cases}$$

where

$$C_{f\alpha} = A_1 P_{f\alpha} + A_{12} X_{f\alpha} - \frac{1}{4}\sum_{f_1=1}^{4} J_{ff_1}(0)P_{f_1\alpha} - \frac{1}{2}\mu_1^\alpha,$$
$$\eta_{f\alpha} = A_{12} P_{f\alpha} + A_2 X_{f\alpha}, \quad f = \overline{1,4}. \tag{4.1}$$

Here we use the notations

$$X_{f\alpha} = \left.\frac{\mathrm{d}X_f}{\mathrm{d}E_\alpha}\right|_{\mathbf{E}=0}, \quad C_{f\alpha} = \left.\frac{\mathrm{d}C_f}{\mathrm{d}E_\alpha}\right|_{\mathbf{E}=0}, \quad \eta_{f\alpha} = \left.\frac{\mathrm{d}\eta_f}{\mathrm{d}E_\alpha}\right|_{\mathbf{E}=0},$$

$$R_{ff_1} = -\frac{2}{\beta Z_4}\sum_{i=1}^{16}\mathrm{e}^{-\beta E_i}\left(\beta^2\frac{\partial E_i^{(1)}}{\partial C_f}\frac{\partial E_i^{(1)}}{\partial C_{f_1}} - \beta\frac{\partial^2 E_i^{(2)}}{\partial C_f \partial C_{f_1}}\right) + \frac{1}{2}\beta P^2,$$
$$M_{ff_1} = -\frac{2}{\beta Z_4}\sum_{i=1}^{16}\mathrm{e}^{-\beta E_i}\left(\beta^2\frac{\partial E_i^{(1)}}{\partial C_f}\frac{\partial E_i^{(1)}}{\partial \eta_{f_1}} - \beta\frac{\partial^2 E_i^{(2)}}{\partial C_f \partial \eta_{f_1}}\right) + \frac{1}{2}\beta PX,$$
$$N_{ff_1} = -\frac{2}{\beta Z_4}\sum_{i=1}^{16}\mathrm{e}^{-\beta E_i}\left(\beta^2\frac{\partial E_i^{(1)}}{\partial \eta_f}\frac{\partial E_i^{(1)}}{\partial \eta_{f_1}} - \beta\frac{\partial^2 E_i^{(2)}}{\partial \eta_f \partial \eta_{f_1}}\right) + \frac{1}{2}\beta X^2,$$

$$A_1 = \frac{X^2}{2\beta Q^3}\ln\frac{1-Q}{1+Q} - \frac{P^2}{\beta Q^2(1-Q^2)},$$
$$A_2 = \frac{P^2}{2\beta Q^3}\ln\frac{1-Q}{1+Q} - \frac{X^2}{\beta Q^2(1-Q^2)},$$
$$A_{12} = -\frac{PX}{2\beta Q^3}\ln\frac{1-Q}{1+Q} - \frac{PX}{\beta Q^2(1-Q^2)},$$

where $E_i^{(1)}$ and $E_i^{(2)}$ are the first and second order (in the fields η_f and C_f) corrections to the eigenvalues E_i, calculated within the perturbation theory. After solving this system of equations, we obtain the static dielectric susceptibility tensor [26]:

$$\chi_{\alpha\beta} = \frac{\mu_\alpha^2(1+\delta_{\alpha z})}{2v}\frac{\delta_{\alpha\beta}}{\frac{-(1-M_\alpha A_{12})^2+N_\alpha A_2+R_\alpha N_\alpha A_{12}}{R_\alpha(1-N_\alpha A_2)+M_\alpha^2 A_2} + A_1 - \frac{1}{4}\nu_\alpha}, \tag{4.2}$$

where $\delta_{\alpha\beta}$ are the Cronecker symbols, $\alpha, \beta = x, y, z$; the following notations are introduced:

$$R_z = R_{11} + 2R_{12} + R_{13}, \quad R_x = R_y = R_{11} - R_{13},$$
$$M_z = M_{11} + 2M_{12} + M_{13}, \quad M_x = M_y = M_{11} - M_{13},$$
$$N_z = N_{11} + 2N_{12} + N_{13}, \quad N_x = N_y = N_{11} - N_{13},$$
$$\nu_x = \nu_y = J_{11}(0) - J_{13}(0), \quad \nu_z = J_{11}(0) + 2J_{12}(0) + J_{13}(0),$$
$$J_{ff_1}(0) = \sum_{\boldsymbol{n}-\boldsymbol{n}_1} J_{ff_1}(\boldsymbol{n}, \boldsymbol{n}_1).$$

In the high-temperature phase, the susceptibility tensor has a simpler form [26]:

$$\bar{\chi}_{\alpha\beta} = \frac{\mu_\alpha^2(1+\delta_{\alpha z})}{2v}\frac{\delta_{\alpha\beta}}{-1/\bar{R}_\alpha + \bar{A}_1 - \frac{1}{4}\nu_\alpha}, \tag{4.3}$$

where

$$\bar{R}_x \equiv \bar{R}_y = \frac{1}{Z_{4p}} \left[\sum_{j=1}^{4} \mathrm{e}^{-\beta E_{pj}} \sum_{i=7}^{8} \frac{(\sqrt{2}U_{2j}U_{7i} + U_{3j}U_{8i})^2}{E_{pj} - E_{pi}} + \sum_{j=7}^{8} \mathrm{e}^{-\beta E_{pj}} \right.$$
$$\times \left(\frac{U_{8j}^2}{E_{pj} - E_{p9}} + \frac{2U_{7j}^2}{E_{pj} - E_{p13}} + \sum_{i=1}^{4} \frac{(\sqrt{2}U_{2i}U_{7j} + U_{3i}U_{8j})^2}{E_{pj} - E_{pi}} \right)$$
$$+ \sum_{j=5}^{6} \frac{\mathrm{e}^{-\beta E_{pj}} U_{6j}^2}{E_{pj} - E_{p9}} + \sum_{i=7}^{8} \frac{\mathrm{e}^{-\beta E_{p13}} 2U_{7i}^2}{E_{p13} - E_{pi}} + \sum_{j=14}^{15} \frac{\mathrm{e}^{-\beta E_{pj}} U_{15j}^2}{E_{pj} - E_{p9}}$$
$$\left. + \mathrm{e}^{-\beta E_{p9}} \left(\sum_{i=5}^{6} \frac{U_{6i}^2}{E_{p9} - E_{pi}} + \sum_{i=7}^{8} \frac{U_{8i}^2}{E_{p9} - E_{pi}} + \sum_{i=14}^{15} \frac{U_{15i}^2}{E_{p9} - E_{pi}} \right) \right],$$

$$\bar{R}_z = \frac{1}{Z_{4p}} \left[\sum_{j=1}^{4} \mathrm{e}^{-\beta E_{pj}} \left(\sum_{i=5}^{6} \frac{(2U_{1j}U_{5i} + U_{3j}U_{6i})^2}{E_{pj} - E_{pi}} \right) \right.$$
$$+ \sum_{j=5}^{6} \mathrm{e}^{-\beta E_{pj}} \left(\sum_{i=1}^{4} \frac{(2U_{1i}U_{5j} + U_{3i}U_{6j})^2}{E_{pj} - E_{pi}} \right) + 2 \sum_{j=7}^{8} \frac{\mathrm{e}^{-\beta E_{pj}} U_{8j}^2}{E_{pj} - E_{p9}}$$
$$\left. + 2 \sum_{i=7}^{8} \frac{\mathrm{e}^{-\beta E_{p9}} U_{8i}^2}{E_{p9} - E_{pi}} + \sum_{j=14}^{15} \frac{\mathrm{e}^{-\beta E_{pj}} U_{15j}^2}{E_{pj} - E_{p9}} + \sum_{i=14}^{15} \frac{\mathrm{e}^{-\beta E_{p9}} U_{15i}^2}{E_{p9} - E_{pi}} \right],$$

$$\bar{A}_1 = A_1|_{P=0} = \frac{1}{2\beta X} \ln \frac{1-X}{1+X}, \quad Z_{4p} = \sum_{i=1}^{16} \mathrm{e}^{-\beta E_{pi}}.$$

In their turn, U_{ij} are components of the matrix H_4^p eigenvectors

$$U_{1i} = \frac{2\Gamma(E_{pi} - \varepsilon)(E_{pi} - w_1)}{\Phi(E_{pi})}, \quad U_{2i} = \frac{2\sqrt{2}\Gamma E_{pi}(E_{pi} - w_1)}{\Phi(E_{pi})},$$
$$U_{3i} = \frac{E_{pi}(E_{pi} - \varepsilon)(E_{pi} - w_1)}{\Phi(E_{pi})}, \quad U_{4i} = \frac{2\Gamma E_{pi}(E_{pi} - \varepsilon)}{\Phi(E_{pi})},$$
$$\Phi(E_{pi}) = (4\Gamma^2(E_{pi} - \varepsilon)^2(E_{pi} - w_1)^2 + E_{pi}^2(8\Gamma^2(E_{pi} - w_1)^2$$
$$+ (E_{pi} - \varepsilon)^2(E_{pi} - w_1)^2 + 4\Gamma^2(E_{pi} - \varepsilon)^2))^{1/2}, \quad i = \overline{1,4};$$
$$U_{5i} = \frac{2\Gamma}{(4\Gamma^2 + E_{pi}^2)^{1/2}}, \quad U_{6i} = \frac{E_{pi}}{(4\Gamma^2 + E_{pi}^2)^{1/2}}, \quad i = 5, 6;$$
$$U_{7i} = \frac{2\Gamma}{(4\Gamma^2 + (E_{pi} - \varepsilon)^2)^{1/2}}, \; U_{8i} = \frac{E_{pi} - \varepsilon}{(4\Gamma^2 + (E_{pi} - \varepsilon)^2)^{1/2}}, \quad i = 7, 8;$$
$$U_{14i} = \frac{2\Gamma}{(4\Gamma^2 + (E_{pi} - w_1)^2)^{1/2}}, \; U_{15i} = \frac{E_{pi} - w_1}{(4\Gamma^2 + (E_{pi} - w_1)^2)^{1/2}}, \quad i = 14, 15.$$

Now we can easily obtain the static dielectric susceptibility tensor

$$\varepsilon_{\alpha\beta} = \varepsilon_\alpha(\infty, T)\delta_{\alpha\beta} + 4\pi\chi_{\alpha\beta}, \quad \alpha, \beta = x, y, z. \tag{4.4}$$

Here $\varepsilon_\alpha(\infty, T)$ is the high-frequency contribution to the susceptibility.

From (4.3) an equation for the Curie-Weiss temperature T_0 follows:

$$\frac{1}{-\bar{A}_1 + \frac{1}{4}\nu_z} + \bar{R}_z = 0. \tag{4.5}$$

Expanding $(4\pi\bar{\chi}_{zz})^{-1}$ in series in temperature near T_0 up to the linear terms, we obtain the Curie-Weiss constant $C_{\rm cw}$ of the high-temperature phase:

$$C_{\rm cw} = 4\pi\frac{\mu_z^2}{v}\frac{1}{(\bar{A}_1 - \frac{1}{4}\nu_z)^2\frac{d}{dT}\left(\frac{1}{-\bar{A}_1+\frac{1}{4}\nu_z} + \bar{R}_z\right)}\Bigg|_{T=T_0}. \tag{4.6}$$

Analytical calculations and thorough analysis performed in [26] show that our results for the Curie-Weiss temperature and constant are correct and do not agree with the results of [8], perhaps because of mistakes or misprints in [8].

In the limit $\Omega \to 0$, the obtained in [26] and presented here results for the components of static dielectric susceptibility tensor yield the corresponding formulas for the KD_2PO_4 type crystals

$$\chi^D_{\alpha\beta} = \frac{\left(\mu^D_\alpha\right)^2(1+\delta_{\alpha z})}{2v_D}\frac{2\beta\mathcal{F}_\alpha\delta_{\alpha\beta}}{\mathcal{D} - \left[\frac{1}{1-P^2} + \beta\frac{\nu^D_\alpha}{4}\right]2\mathcal{F}_\alpha}, \tag{4.7}$$

where

$$\mathcal{D} = 4\mathrm{e}^{-\beta w}\mathrm{ch}\beta C + 2\mathrm{e}^{-\beta\varepsilon} + \mathrm{e}^{-\beta w_1} + \mathrm{ch}2\beta C,$$

$$\mathcal{F}_x = \mathcal{F}_y = \mathrm{e}^{-\beta\varepsilon} + \mathrm{e}^{-\beta w}\mathrm{ch}\beta C, \quad \mathcal{F}_z = \mathrm{e}^{-\beta w}\mathrm{ch}\beta C + \mathrm{ch}2\beta C - P^2\mathcal{D}.$$

The longitudinal susceptibility χ^D_{zz} accords with the results of [14–16], whereas the transverse components χ^D_{xx}, χ^D_{yy} accord with the results of [18]. In addition, the transverse components do agree at $T > T_{\rm c}$ with the calculations of [29] but do not agree at $T < T_{\rm c}$ because of the neglected in [29] intercluster correlations. Neglecting ν_x and ν_y from (4.7) we obtain the results of [12–15] for the transverse susceptibility.

Hence, to calculate the components of static dielectric susceptibility tensor we need to find numerically the eigenvalues and eigenfunctions of the matrix (2.6), find corrections $E_i^{(1)}$ and $E_i^{(2)}$, calculate the coefficients R_{ff_1}, M_{ff_1}, N_{ff_1}, and, finally, to calculate the tensor components, using the results of numerical solution of the system of equations for X and P.

5. Discussion

In this section we shall verify how the presented theory describes experimental data for thermodynamic and static dielectric characteristics of the KDP type ferroelectrics. Our main task is, using the fitting procedure proposed by us in [26], to determine optimal values of the theory parameters for the RbH_2PO_4, KH_2AsO_4,

RbH_2AsO_4 crystals, which would provide a good quantitative agreement with the experiment, as we did in [26] for a KH_2PO_4 crystal. We use the experimental data presented in table 1, as well as those shown in the figures below. For comparison, we also calculate the corresponding physical characteristics of the studied crystals using the values of the theory parameters given in other papers. The obtained optimal values of the theory parameters as well as those of other authors are presented in table 2. We would like to remind that the entire set of the model parameters – Ω, ε, w, ν_z for each crystal was chosen such that the best agreement of theoretical and experimental results for the Curie T_c and Curie-Weiss T_0 temperatures, temperature dependence of polarization $\mathcal{P}(T)$, polarization jump $\mathcal{P}_c = \mathcal{P}(T_c)$, and saturation polarization $\mathcal{P}_s = \mathcal{P}(T_s)$ was obtained. Finally, from the found sets of the parameters we selected those providing the best fit to experimental temperature dependence of the proton contribution to the specific heat $\Delta C(T)$, considering also an agreement with the experimental values of the transition entropy $S_c = S(T_c + 0)$ and entropy jump at the transition point $\Delta S_c = S(T_c + 0) - S(T_c - 0)$. The above quantities were calculated from equations (3.2), (3.3), (3.5), (3.6) and (4.5), whereas the specific heat was found by numerical differentiation of entropy (3.2) with respect to temperature. Then, the static dielectric characteristics were calculated with the thus obtained parameters. Experimental temperature dependence of the primitive cell volume of the crystals was approximated by the formula

$$v(T) = v\theta(T_c - T) + \bar{v}\theta(T - T_c),$$

where $\theta(T)$ is the step function, whereas v and $\bar{v}$ are the cell volumes in the ferroelectric and paraelectric phases, presented in table 1. Such an approximation of the dependence $v(T)$ is rather good because of a weak temperature dependence of the lattice constants in these crystals [57,59]. Due to the absence of the required experimental data, for KH_2AsO_4 and RbH_2AsO_4 we take $v = \bar{v}$.

It should be noted that the fitting procedures in order to describe the phase transition and behaviour of the physical characteristics of the KDP type crystals were performed in several papers, two of which [8] and [10] are the most noteworthy. In the first one, a criterion for setting the theory parameters was to obtain an agreement of the theoretical values of $\sqrt{\Delta S(\tau)/S_c}$ ($S_c = S(T_c + 0)$, $\Delta S(\tau) = S_c - S(\tau)$, $\tau = 1 - T/T_c$) and the values for these quantities calculated from the experimental data for the specific heat. The utmost attention was paid to the temperature interval near T_c ($\tau \leqslant 0.005$), where the error in the quantity $\sqrt{\Delta S(\tau)/S_c}$ calculated from the experimental data for the specific heat is the smallest. Experimental data for temperature dependences of other physical characteristics of the KH_2PO_4 family crystals in [8] were not studied. Later we shall estimate the efficiency of such an approach. In [10] some of the values of the theory parameters found in [8] were corrected in order to obtain a better theoretical description of polarization. The results of [10] will be also discussed later.

The efficiency of the approach to setting the theory parameters [26] used in the present paper is seen in figures 2, 3, 6, and tables 1, 2. As one can see, the set of the model parameters for the KH_2PO_4 crystal [26] (number 1 in table 2) provides

Table 1. Experimental data for the KDP type crystals.

	KH_2PO_4	RbH_2PO_4	KH_2AsO_4	RbH_2AsO_4
T_c, K	122.88 [30] 122.7 [34] 122.25 [37] 123 [40]	146.8 [31] 147 [35] 147.1 [32] 147.7 [41]	95.57 [32] 96.15 [36] 96.2 [38] 96.26 [42]	109.75[33] 109.9 [32] 110.0 [39] 110.25 [42]
$T_c - T_0$, K	0.05 [13,34] 0.06 [43,44] 0.07 [45] 0.026 [47]	–	1.9 [36] 2.6 [42]	0.04[42] 0.05 [39] 0.2 [46]
$\mathcal{P}_c$, 10^{-2} C/m^2	1.8 [44] 1.87 [49]	1.6 [48]	4.5 [39]	3.8 [39] 3.7 [46]
$\mathcal{P}_s$, 10^{-2} C/m^2	5.0 [37] 5.1 [50]	–	5.25 [39]	5.4 [33] 5.0 [39]
S_c, molec.$^{-1}$	0.39 [34] 0.40 [51] 0.422 [52]	0.358 [31] 0.488 [9] 0.50 [8]	0.506 [36] 0.509 [39]	0.502 [33] 0.468 [39] 0.53 [8]
ΔS_c, molec.$^{-1}$	0.0456 [51] 0.0469 [53]	–	0.129 [36] 0.377 [39]	0.2702 [39]
C_{cw}, K	2856 [10] 2925 [37] 3000 [40] 3200 [34]	2924 [41] 3020 [54] 3060 [35] 3200 [55]	2350 [39] 2700 [42]	2580 [42] 2732 [46] 3100 [39]
v, 10^{-30} m^3	189.635 [56]	208.674 [57]	–	–
$\bar{v}$, 10^{-30} m^3	191.127 [58]	208.724 [57]	205.249 [59]	223.592 [59]

Table 2. The found sets of the model parameters Ω, ε, w, ν_z, ν_x etc. for the KDP type crystals along with the data of other sources and the physical characteristics calculated with these parameters.

N	w, K	ε, K	Ω, K	ν_z, K	T_c, K	$T_c - T_0$, K	P_c/P_s
1_{KDP}	**600**	**55**	**138**	**109.22**	**122.751**	**0.042**	**0.360**
2 [8]	550	61	74	68	122.178	0.021	0.37
3 [8]	570	64	81	64	123.414	0	0
4 [14]	750	50	250	202.4	121.966	0.063	0.339
5 [14]	952	52	300	213.6	122.053	0.074	0.357
6 [10]	558	62	97	74.4	122.617	0	0
7_{RDP}	**565**	**60.85**	**145**	**154.81**	**147.103**	**0.030**	**0.30**
8 [8]	550	72	77	88	145.218	0	0.01
9 [10]	675	75	121	90	147.476	0	0
10_{KDA}	**420**	**33**	**55**	**89.2**	**96.194**	**1.611**	**0.852**
11 [8]	490	44	33	52	95.098	0.716	0.869
12 [10]	449	41	38	65.2	97.067	0.883	0.842
13_{RDA}	**415**	**39.5**	**56**	**102.3**	**110.004**	**0.964**	**0.751**
14 [8]	500	52	48	64	110.728	0.306	0.695

a very good description of the chosen experimental data, much better than the sets found in other papers.

Choosing the values of the theory parameters for the RbH_2PO_4 crystal, we took into account the experimental data of [9] ($\mathcal{P}_c/\mathcal{P}_s = 0.30$) and described the phase transition of the first but very close to the second order, using the experimental data for polarization [15]. Unfortunately, the experimental data for $T_c - T_0$ for this crystal are not available; therefore, we can say nothing about the agreement with the experiment for this quantity. The results of the fitting procedure for the RbH_2PO_4 crystal are shown in figures 2, 4 and in tables 1, 2. As one can see, the obtained set 7 provides a very good quantitative description of experimental data, overall better than the sets 8 and 9, even though the set 9 provides a fair agreement with the experimental specific heat as well.

Table 2. The found sets of the model parameters for the KDP type crystals (continuation).

N	S_c, molec.$^{-1}$	ΔS_c, molec.$^{-1}$	$\mathcal{P}_c \cdot 10^2$, C/m^2	$\mathcal{P}_s \cdot 10^2$, C/m^2	$\mu_z \cdot 10^{30}$, C $\cdot$ m	$\bar{\mu}_z \cdot 10^{30}$, C$\cdot$ m
1	**0.4571**	**0.0576**	**1.824**	**5.069**	**5.017**	**5.856**
2	0.4877	0.0634	1.876	5.069	4.853	–
3	0.4784	0	0	5.069	4.860	–
4	0.2726	0.0287	1.718	5.069	6.112	–
5	0.1883	0.0234	1.810	5.069	6.622	–
6	0.4844	0	0	4.902	4.734	–
7	**0.5289**	**0.0438**	**1.510**	**5.015**	**5.481**	**6.449**
8	0.5560	0	0.062	4.776	5.033	–
9	0.4821	0	0	4.808	5.117	–
10	**0.5057**	**0.3474**	**4.463**	**5.238**	**5.422**	**5.979**
11	0.4440	0.3257	4.479	5.155	5.301	–
12	0.4793	0.3243	4.369	5.189	5.343	–
13	**0.5618**	**0.2890**	**3.868**	**5.15**	**5.809**	**6.509**
14	0.4854	0.2219	3.528	5.076	5.702	–

Table 2. The found sets of the model parameters for the KDP type crystals (continuation).

N	ν_x, K	$\mu_x \cdot 10^{30}$, C · m	$\varepsilon_x(\infty)$	$\bar{\varepsilon}_x(\infty)$	$T_{\rm s}$, K
1	**40**	**13.078**	**12.6**	**26.5**	**62.56**
2	0	13.672	13	25	61.09
4	0	15.475	2.5	20.2	76.91
5	0	16.320	0	17.6	83.73
7	**60**	**14.171**	**15.4**	**21.8**	**72.03**
9	0	15.934	16.5	18.2	72.81
10	**30**	**16.950**	**14.5**	**22**	**49.38**
12	0	19.074	15	15	50.16

Figures 2, 5 illustrate the obtained theoretical description of the KH_2AsO_4 and RbH_2AsO_4 crystals. A disagreement between the experimental data of [33,39] for polarization $\mathcal{P}(T)$ of RbH_2AsO_4crystal takes place, because of the very different values of saturation polarization $\mathcal{P}_{\rm s}$ (see table 1). Since the saturation polarization in RbH_2PO_4 is smaller than that in KH_2PO_4, we took for $\mathcal{P}_{\rm s}$ of RbH_2AsO_4 the data of [39] and removed, thereby, the disagreement. As one should expect, for the obtained sets of the theory parameters 10 and 13 we have a very good agreement of theoretical and experimental results. It should be noted that the theoretical data obtained for the sets 11 and 12 provide a much worse description of experimental specific heat of KH_2AsO_4 than the set 10. The theoretical curves calculated with the set 14 for the RbH_2AsO_4 crystal accord with experiment fairly well, but worse than the results obtained with the set 13. We would like to mention that these values of the model parameters for the KH_2AsO_4 and RbH_2AsO_4 crystals were found using the experimental data for polarization, obtained in [33,36,39] from the approximate formula $\mathcal{P}(T)/\mathcal{P}_{\rm s} = \sqrt{\Delta S(T)/S_{\rm c}}$ that corresponds to the Landau expansion of the free energy with only quadratic in polarization terms taken into account. Since here the clear first order phase transition takes place, we have some doubts about a high precision of these experimental data. Values of polarization obtained from the hysteresis loops or electrocaloric measurements would be more valuable.

Let us verify how the found values of the theory parameters in the present paper describe the quantity $\sqrt{\Delta S(\tau)/S_{\rm c}}$ – the criterion used in the fitting procedure proposed in [8]. As seen in figure 6, for the KH_2PO_4 and RbH_2AsO_4 crystals the sets 1

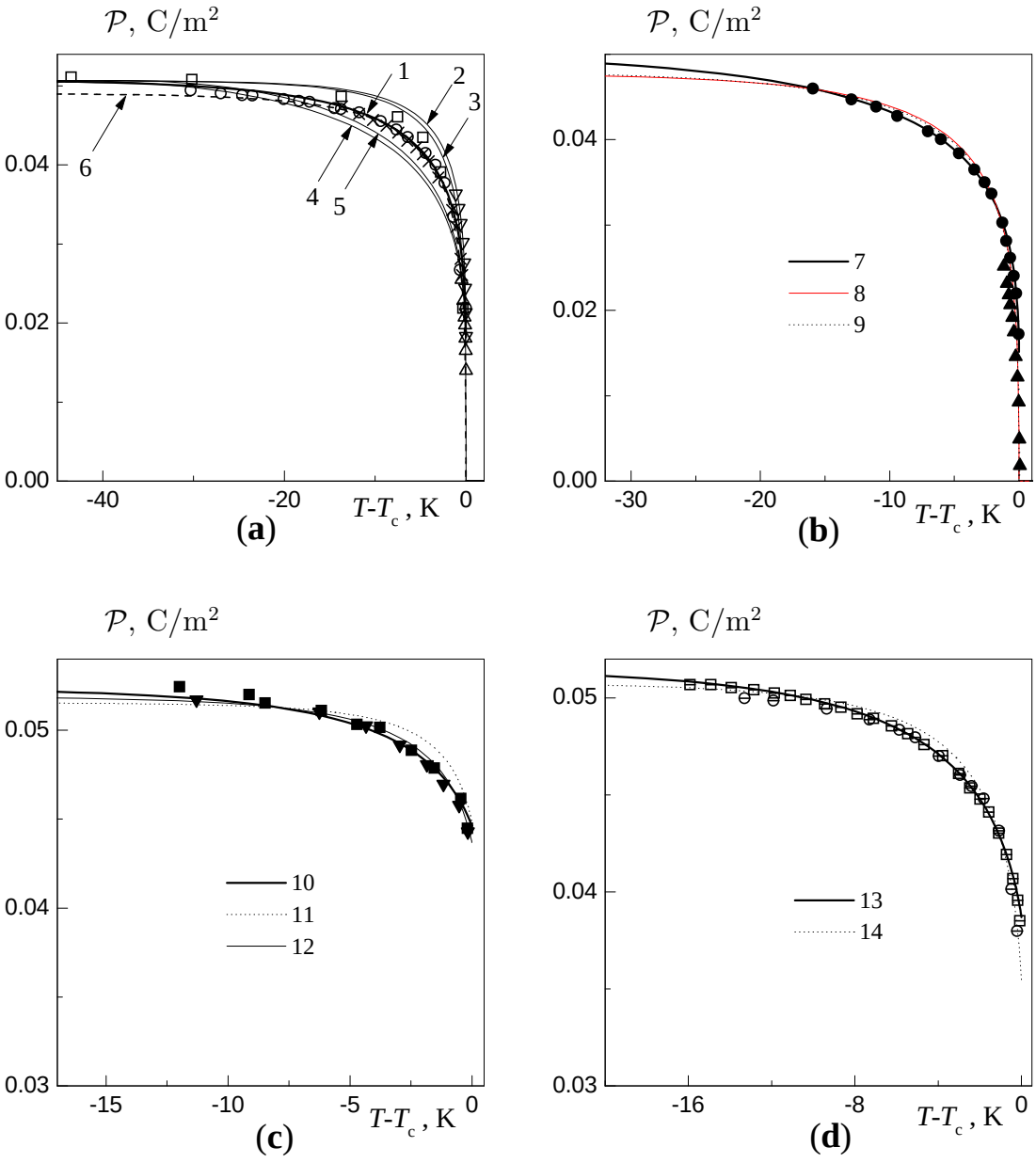

Figure 2. Temperature dependence of spontaneous polarization of the KH_2PO_4 (a), RbH_2PO_4 (b), KH_2AsO_4 (c), RbH_2AsO_4(d) crystals. Lines are theoretical results for the sets of the model parameters: 1–6 (a), 7–9 (b), 10–12 (c), 13, 14 (d), given in table 2. Points are experimental data taken from ○ – [37], □ – [60], ▽ – [49], △ – [43], × – [15] (a); ● – [15], ▲ – [31] (b); ▼ – [15], ■ – [36] (c); ⊖ – [39], ⊟ – [33] (d).

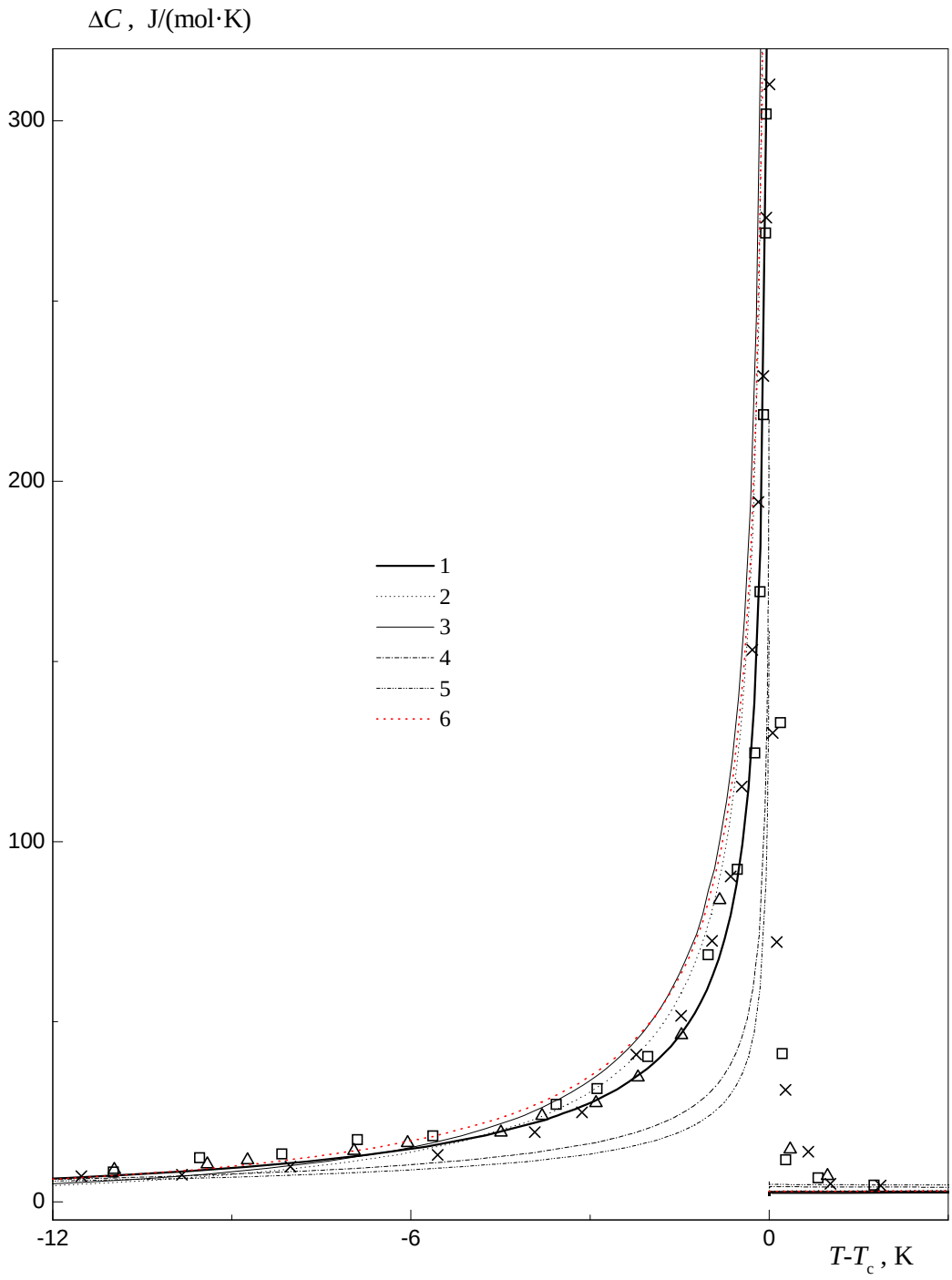

Figure 3. Temperature dependence of the proton contribution to the specific heat of the KH_2PO_4 crystals. Lines are theoretical results for the sets 1–6 of the theory parameters given in table 2. Points are experimental data taken from □ – [30], △ – [34], × – [52].

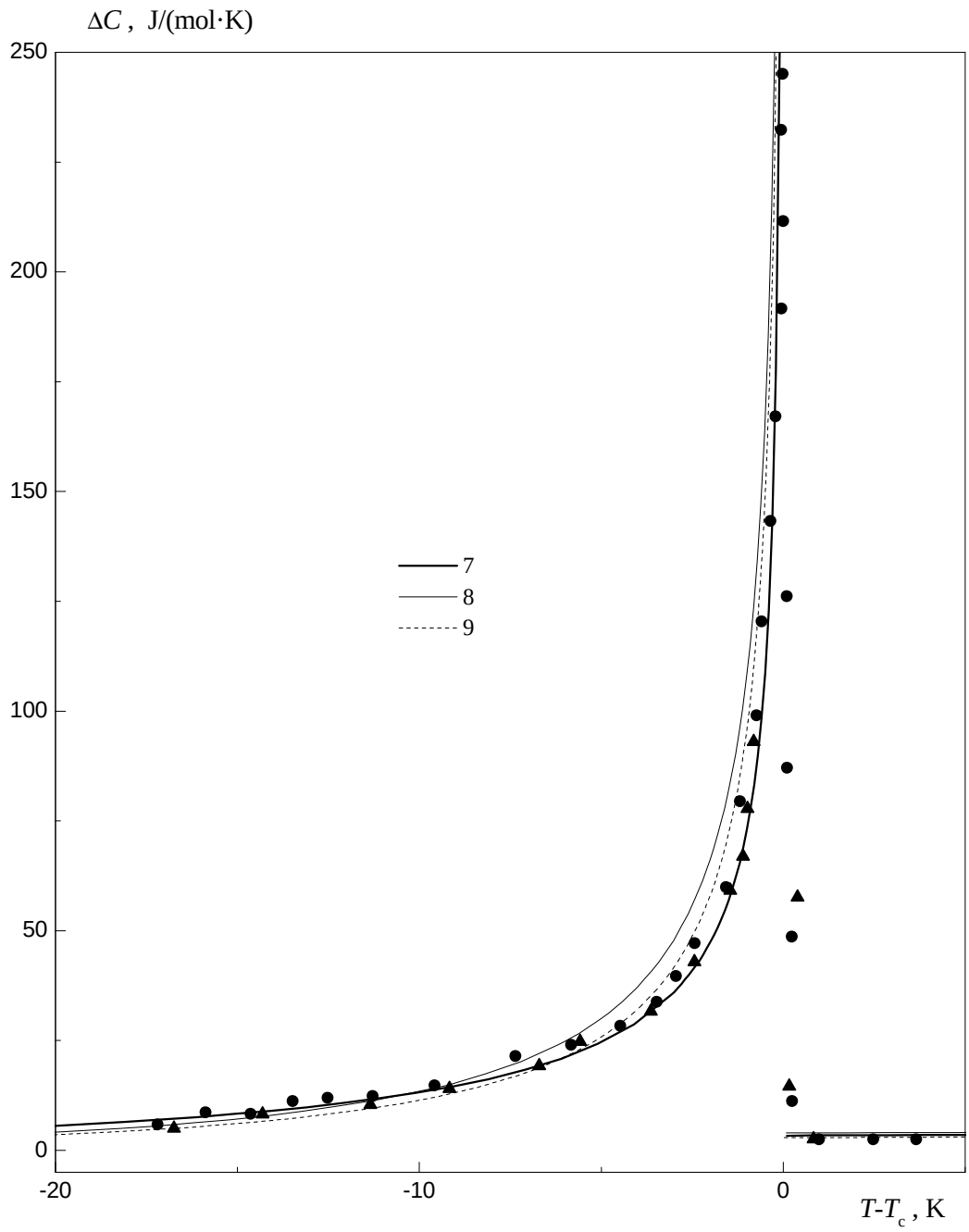

Figure 4. Temperature dependence of the proton contribution to the specific heat of the RbH_2PO_4 crystal. Lines are theoretical results for the sets 7–9 of the theory parameters given in table 2. Points are experimental data taken from ● – [41], ▲ – [31].

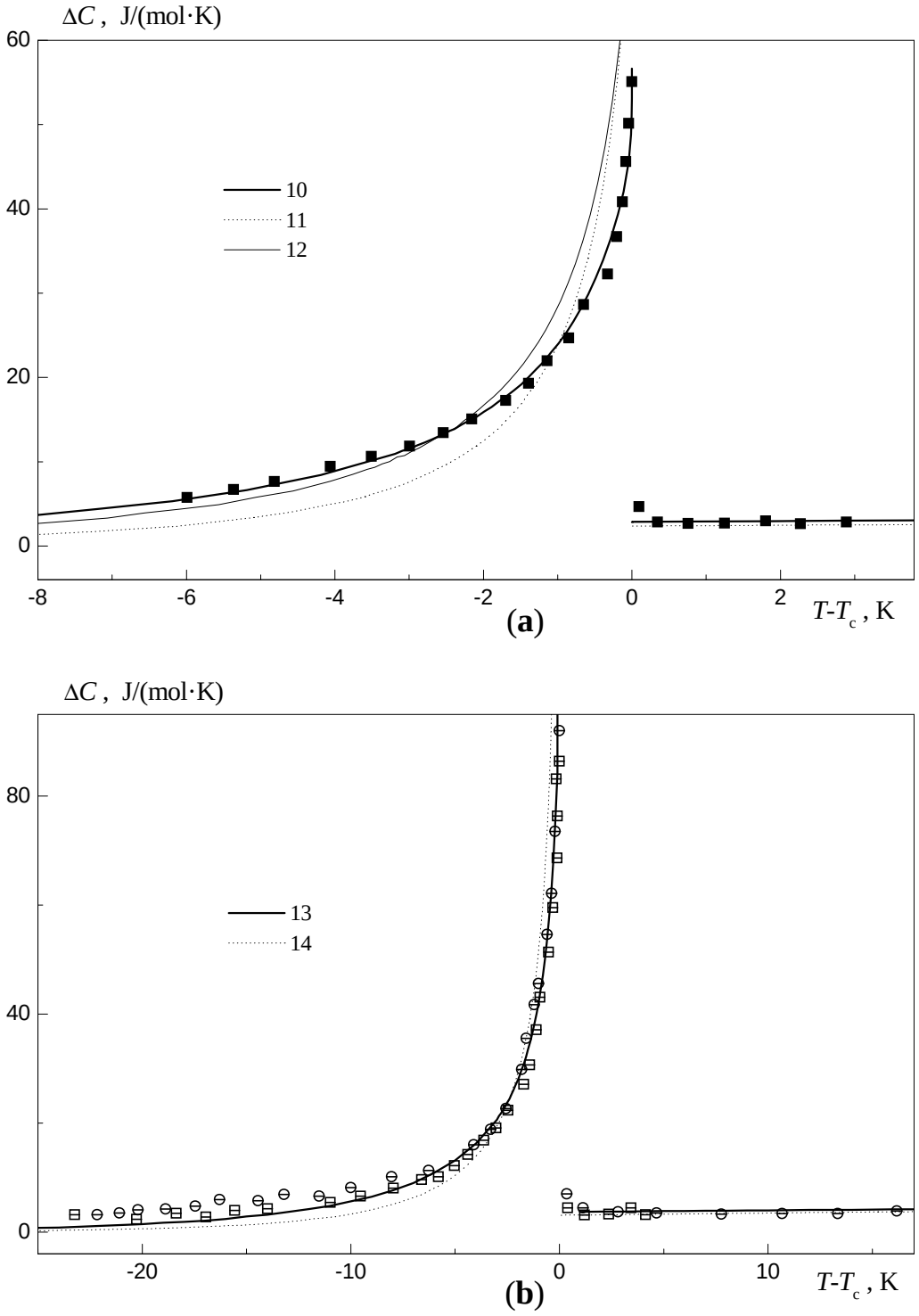

Figure 5. Temperature dependence of the proton contribution to the specific heat of the KH_2AsO_4 (a) and RbH_2AsO_4 (b) crystals. Lines are theoretical results for the sets of the theory parameters 10–12 (a) and 13, 14 (b) given in table 2. Points are experimental data taken from ■ – [36], ⊖ – [39], ⊟ – [33].

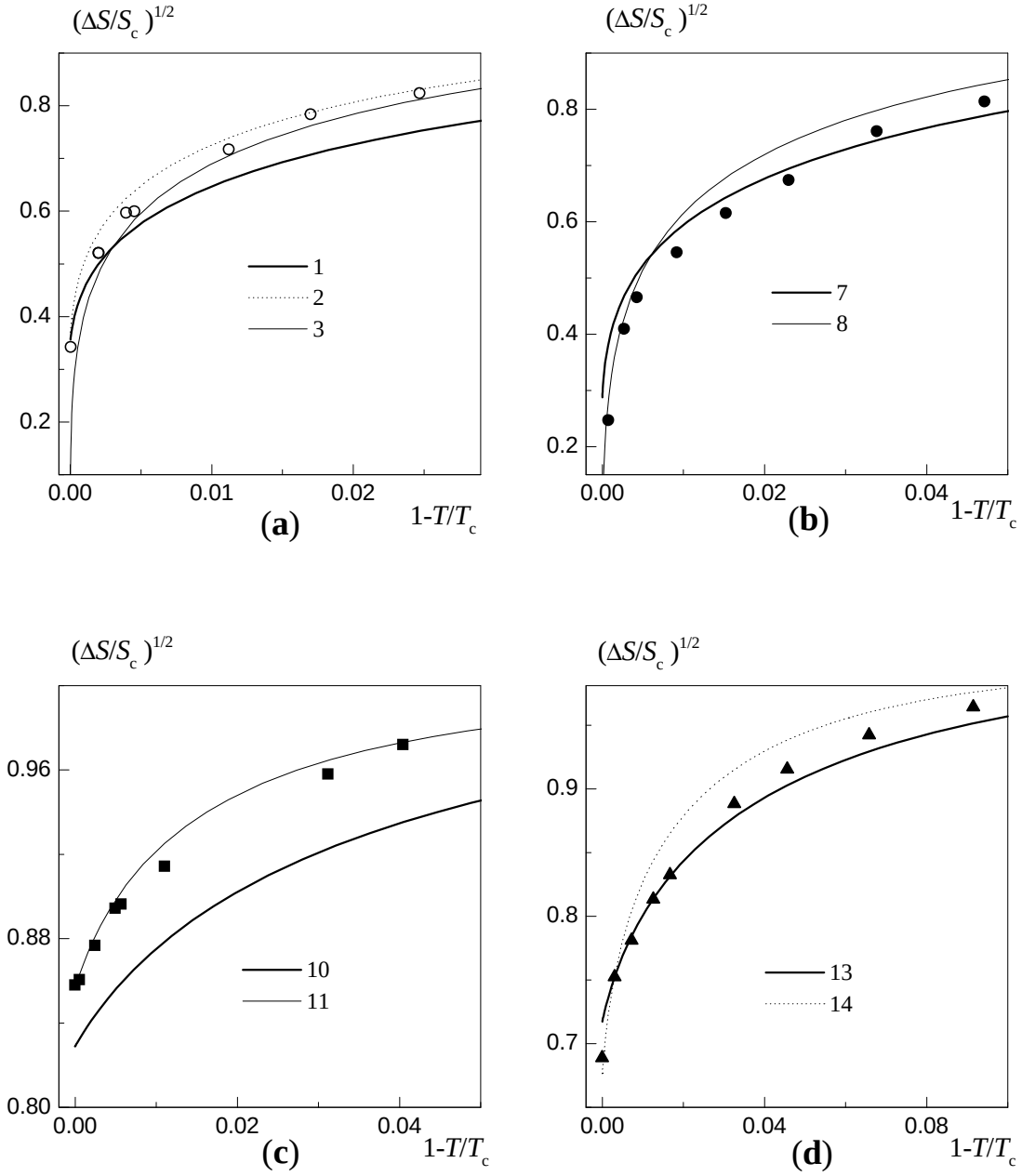

Figure 6. Temperature dependence of entropy change $(\Delta S/S_c)^{1/2}$ ($\Delta S = S(T) - S(T_c+0)$, $S_c = S(T_c+0)$) for the crystals KH_2PO_4 (a), RbH_2PO_4 (b), KH_2AsO_4 (c), and RbH_2AsO_4 (d). Lines are theoretical results for the sets 1–3 (a); 7, 8 (b); 10, 11 (c); and 13, 14 (d) of the model parameters given in table 2. ○, ●, ■, ▲ are data taken from [8].

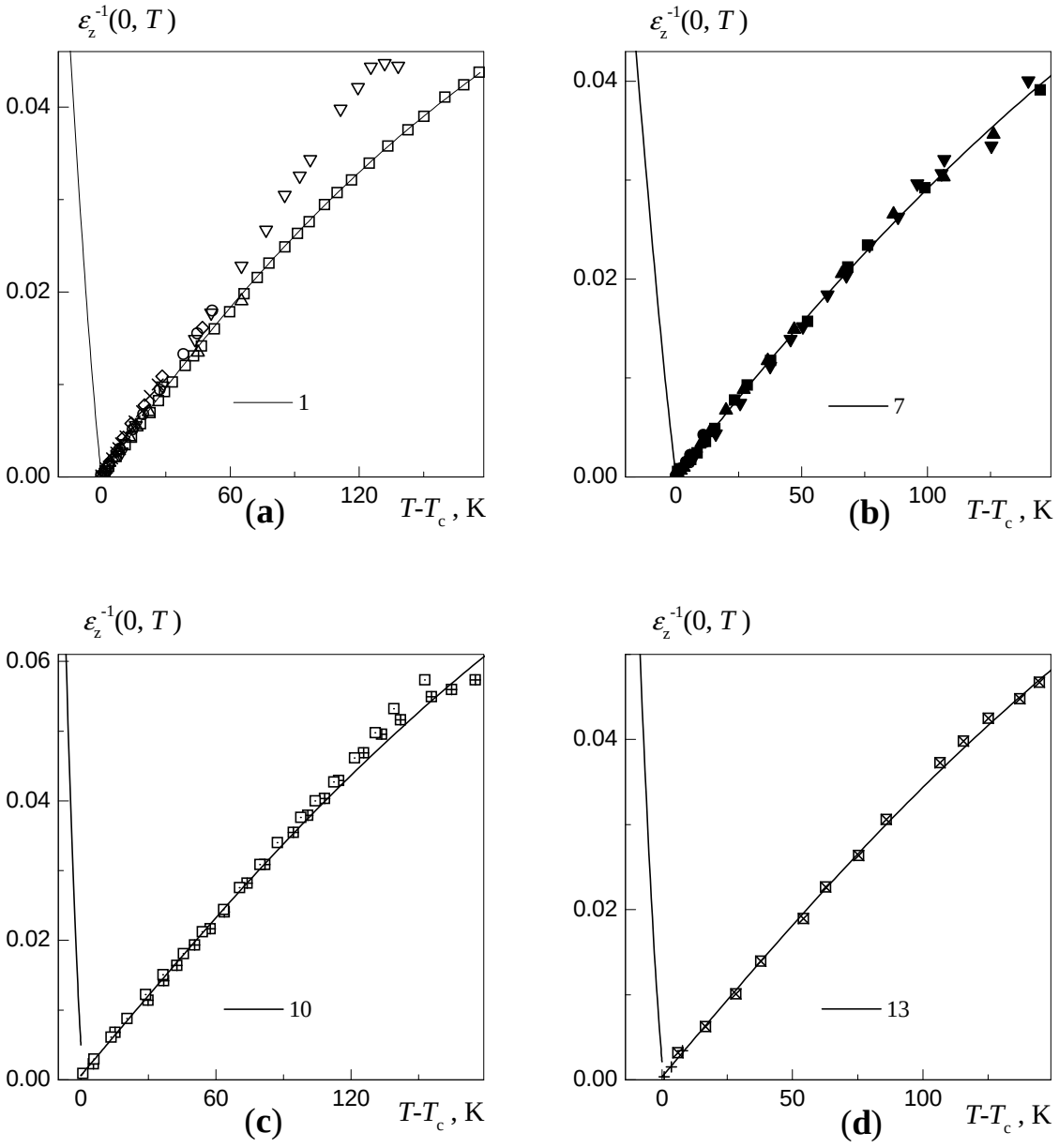

Figure 7. Temperature dependence of the inverse static dielectric permittivity of the KH_2PO_4 (a), RbH_2PO_4 (b), KH_2AsO_4 (c), and RbH_2AsO_4 (d) crystals. Lines are theoretical results for the sets of the model parameters of table 2: the set 1 with $\varepsilon_z(\infty) = 6.7$, $\bar{\varepsilon}_z(\infty) = 9$ (a); the set 7 with $\varepsilon_z(\infty) = \bar{\varepsilon}_z(\infty) = 7$ (b); the set 10 with $\varepsilon_z(\infty) = \bar{\varepsilon}_z(\infty) = 5$ (c); the set 13 with $\varepsilon_z(\infty) = \bar{\varepsilon}_z(\infty) = 5.6$ (d). Points are experimental data taken from ○ – [37], □ – [62], ▽ – [63], △ – [34], × – [64], ◇ – [65] (a); ▲ – [35], ▼ – [63], ■ – [66], ● – [54] (b); ⊞ – [63], ⊡ – [57] (c); + – [42], ⊠ – [63] (d).

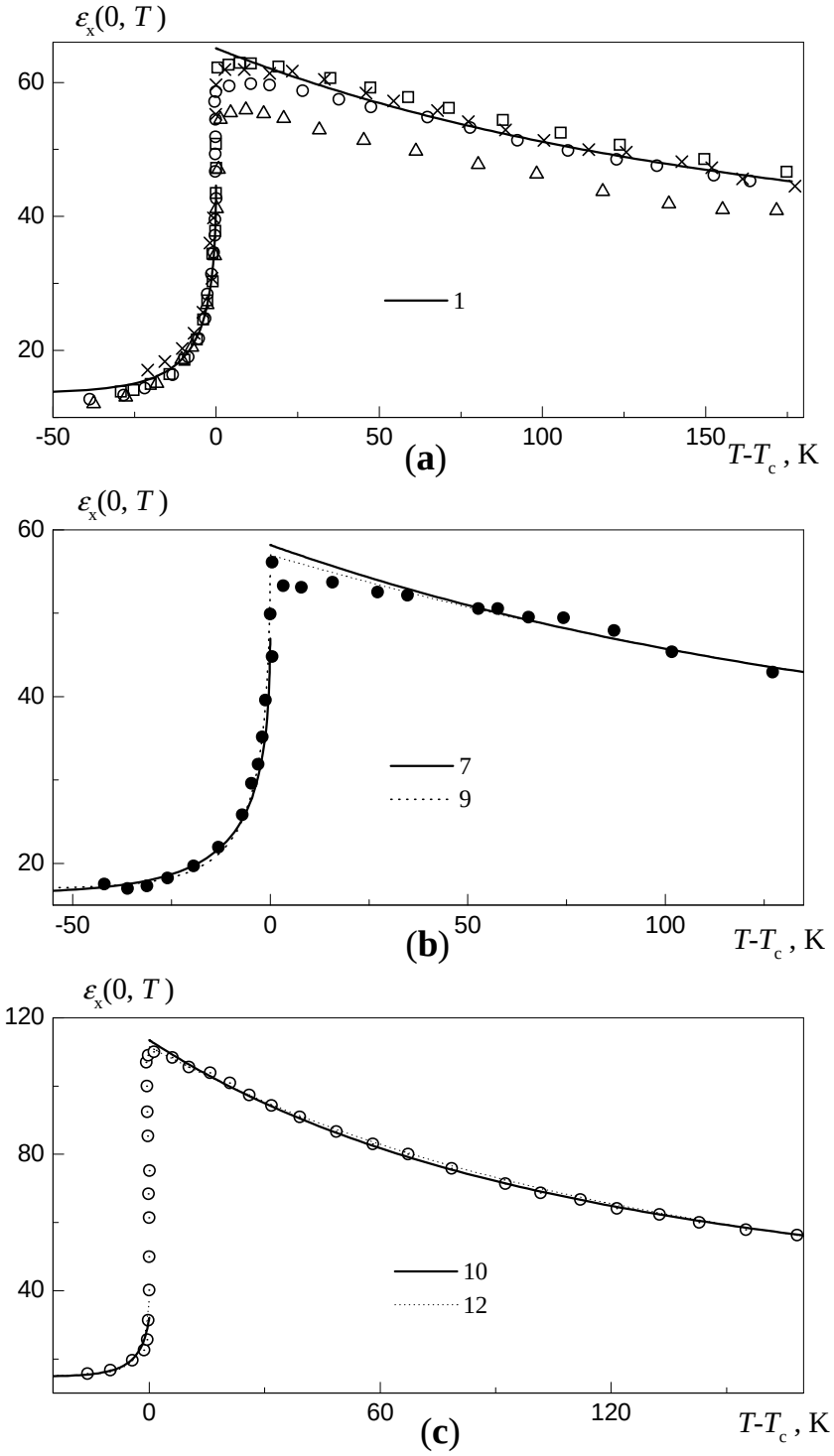

Figure 8. Temperature dependence of the static transverse dielectric permittivity of the KH_2PO_4 (a), RbH_2PO_4 (b), and KH_2AsO_4 (c) crystals. Lines are theoretical results for the sets: 1 (a); 7, 9 (b); 10, 12 (c) given in table 2. Points are experimental data taken from ○ – [12], □ – [62], △ – [67], ×, ●, ⊙ – [15].

and 13 of the model parameters found in this paper provide a better agreement with the experiment than the sets 2, 3, 14 (taken from [8]) exactly in the required region. Our parameters 7 for the RbH_2PO_4 crystal obey this criterion a little worse – a good agreement is obtained at $0.01 \leqslant \tau \leqslant 0.05$ (see figure 6); whereas for KH_2AsO_4 parameters 10 do not obey the criterion at all (see figure 6). Taking into account the above facts and the presented results of theoretical calculations, we may conclude that the approach accepted in the present paper which uses direct experimental data is the most efficient and consistent approach that permits to find an optimal set of the model parameters.

Let us now explore the theoretical dependences of the dielectric characteristics of the crystals (4.4) using the above chosen values of the model parameters. For the high-frequency contribution to the permittivity, which as indicated by the results obtained in [16,18,61] is nearly temperature independent, we use a simple approximation

$$\varepsilon_\alpha(\infty, T) = \varepsilon_\alpha(\infty)\theta(T_\mathrm{c} - T) + \bar{\varepsilon}_\alpha(\infty)\theta(T - T_\mathrm{c}),$$

whereas the values of $\varepsilon_\alpha(\infty)$ and $\bar{\varepsilon}_\alpha(\infty)$ were determined by fitting the theoretical results to the experimental data for the permittivity. The longitudinal effective dipole moment $\bar{\mu}_z$ of the crystals was determined from the formula (4.6) for the Curie-Weiss constant (the temperature derivatives were evaluated numerically as $G(T_0 + 10\,\mathrm{K})/10\,\mathrm{K}$). Using the experimental values of the Curie-Weiss constant, though very different in different sources (see table 1), to set $\bar{\mu}_z$ we took the following values: in KH_2PO_4 – 2920 K, in RbH_2PO_4 – 3010 K, in KH_2AsO_4 – 2550 K, in RbH_2AsO_4 – 2700 K. The constant high-frequency contribution $\bar{\varepsilon}_\alpha(\infty)$ was determined by fitting to the experimental data for $\varepsilon_z(0, T)$ in a wide temperature interval above the T_c; for the KH_2PO_4 we used the data of [62] only. As one can see in figure 7, a very good theoretical description of the experimental permittivity of the RbH_2PO_4, KH_2AsO_4, RbH_2AsO_4 crystals is obtained. For the low-temperature region we present only the theoretical results, because of the absence of reliable experimental data for single-domain samples.

Figure 8 shows the theoretical description of experimental data for the transverse dielectric permittivity $\varepsilon_x(0, T)$. Values of μ_x, $\varepsilon_x(\infty)$, and $\bar{\varepsilon}_x(\infty)$ for each set of the model parameters (see table 2) were chosen such as to obtain the best fit to the experiment. There is also the parameter ν_x, the increase of which raises up $\varepsilon_x(0, T_\mathrm{c} + 0)$ (see [26]) and this fact was taken into account. From the figures we see that the error in the description of the experimental data does not exceed 2% at all temperatures except for the dome-shaped region near T_c, where the error reaches 8%. The experimental data of [67] for the transverse permittivity of KH_2PO_4 above the Curie temperature, for unknown reasons lie much lower than the data of [12,15,62]. Therefore, to obtain a good fit to the points of [67], we need to use the values of μ_x and $\bar{\varepsilon}_x(\infty)$ rather smaller than those chosen before. For the crystals RbH_2PO_4 and KH_2AsO_4, the values of the model parameters of [10] also provide a good agreement with the experiment. This proves that the dielectric characteristics cannot be a criterion for setting the model parameters $\Omega, \varepsilon, w, \nu_z$. Data for the transverse permittivity of RbH_2AsO_4 are not available; therefore we did not study it theoretically.

As mentioned in [5,7,68], the cluster approximation for the proton model yields the unphysical behaviour of polarization and specific heat at low temperatures. The character of the low temperature behaviour of these and of dielectric characteristics was studied in [26,69], where we noted that with the increase of the tunnelling integral Ω, the unphysical behaviour emerges at higher temperatures. On decreasing the temperature, the unphysical behaviour manifests first in the free energy and entropy, then in polarization, specific heat and dielectric permittivity. At large tunnelling, the unphysical behaviour appears at 1–2 K above the temperature at which entropy changes its sign to a negative. In addition, the unphysical behaviour itself can have a character of the phase transition (see [69]). As far as the unphysical behaviour of thermodynamic and dielectric characteristics for the other sets of the model parameters $\Omega, \varepsilon, w, \nu_z, \nu_x$ presented in table 2 is concerned, for polarization it appears below the temperature $T_{\rm s}$ of polarization saturation (see table 2), whereas for the free energy and entropy it appears at 15–25 K higher [69]. We can assuredly maintain that for the found sets of the model parameters the region of physically incorrect behaviour of the system emerges at temperatures not higher than 40 K below the Curie temperature.

6. Conclusions

In this paper, the proton ordering model with tunnelling is used for a description of experimental thermodynamic and dielectric characteristics of ferroelectric KH_2PO_4, RbH_2PO_4, KH_2AsO_4, RbH_2AsO_4 crystals. The proposed in [26] numerical method of an unambiguous setting of optimal values of the model parameters Ω, ε, w, ν_z is applied for a theoretical investigation of the physical characteristics of all the KDP type crystals. The values of the model parameters, found using the experimental data for temperature dependences of polarization and specific heat, Curie and Curie-Weiss temperatures, transition entropy and entropy jump at the transition point, provide a good quantitative description of the longitudinal and transverse components of dielectric permittivity.

We obtained that for all the crystals, the model yields a very good quantitative agreement between experimental data and theoretical results. Therefore, we may conclude that the role of striction, correlations and other effects is not that essential as maintained in [7,8]. The obtained results suggest that the tunnelling effects in the KH_2PO_4 and RbH_2PO_4 crystals are much more significant than in KH_2AsO_4 or RbH_2AsO_4. Therefore, without taking into account tunnelling, the description of experimental data for KH_2PO_4 and RbH_2PO_4 cannot be very good.

Undoubtedly, it is interesting and necessary to expand the proton ordering model with tunnelling in order to describe the influence of lattice deformations, external fields, and other effects in undeuterated KDP type crystals, as it was done in [70–72] for deuterated DKDP type ferroelectrics. This will be a subject of our forthcoming studies.

References

1. Blinc R. // J. Phys. Chem. Solids, 1960, vol. 13, No. 3, p. 204–211.
2. De Gennes P.G. // Solid State Commun., 1963, vol. 1, No. 6, p. 132–137 .
3. Tokunaga M., Matsubara T. // Prog. Theor. Phys., 1966, vol. 35, No. 4, p. 581–599.
4. Kobayashi K.K. // J. Phys. Soc. Japan, 1968, vol. 24, No. 3, p. 497–508.
5. Blinc R., Svetina S. // Phys. Rev., 1966, vol. 147, p. 423–438.
6. Levitsky R.R., Korinevsky N.A., Stasyuk I.V. // Ukr. Fiz. Zhurn., 1974, vol. 19, No. 8, p. 1289–1297 (in Russian).
7. Vaks V.G., Zinenko V.I. // Zhurn. Eksper. i Theor. Fiz., 1973, vol. 64, No. 2, p. 650–664 (in Russian).
8. Vaks V.G., Zein N.E., Strukov B.A. // Phys. Stat. Sol. (a), 1975, vol. 30, p. 801–819.
9. Fairall C.W., Reese W. // Phys. Rev. B, 1975, vol. 11, No. 5, p. 2066–2068.
10. Chabin M., Gilletta F. // Ferroelectrics, 1977, vol. 15, p. 149–154.
11. Havlin S., Litov E., Uehling E.A. // Phys. Rev. B, 1974, vol. 9, No. 3, p. 1024–1028.
12. Havlin S., Litov E., Sompolinsky H. // Phys. Lett., 1975, vol. 51A, No. 1, p. 33–35.
13. Havlin S., Litov E., Sompolinsky H. // Phys. Rev. B, 1976, vol. 13, No. 11, p. 4999–5006.
14. Havlin S. // Ferroelectrics, 1987, vol. 71, p. 183–223.
15. Gilletta F., Chabin M. // Phys. Stat. Sol. (b), 1980, vol. 100, p. k77–k82.
16. Levitsky R.R., Zachek I.R., Mits Ye.V. Preprint ITF–87–114P, Kiev, 1987, 48 p. (in Russian).
17. Levitsky R.R., Zachek I.R., Mits Ye.V. – In: Proc. Contributed papers of Conf. on Modern problems of statistical physics. Vol. 2, Lviv, 3–5 February 1987, p. 194–206 (in Russian).
18. Levitsky R.R., Zachek I.R., Mits Ye.V. Preprint ITF–87–115P, Kiev, 1987, 48 p. (in Russian).
19. Zachek I.R., Mits Ye.V., Levitsky R.R. Preprint ITF–89–7P, Kiev, 1989, 45 p. (in Russian).
20. Tokunaga M., Tatsuzaki I. // Phase Trans., 1984, vol. 4, p. 97–156.
21. Tominaga Y. // Ferroelectrics, 1983, vol. 52, p. 91–100.
22. Tokunaga M., Matsubara T. // Ferroelectrics, 1987, vol. 72, p. 175–191.
23. Tokunaga M. // Progr. Theor. Phys. Suppl., 1984, vol. 80, p. 156–162.
24. Stasyuk I.V., Ivankiv Ya.L. Preprint ITF–87–57P, Kiev, 1987, 25 p. (in Russian).
25. Blinc R. // Z. Naturforsch., 1986, vol. 41a, p. 249–259.
26. Levitskii R.R., Lisnii B.M. Preprint of the Institute for Condensed Matter Physics, ICMP–01–9U, Lviv, 2001, 51 p. (in Ukrainian).
27. Korinevsky N.A. / Preprint ITF–80–71P, Kiev, 1980, 22 p. (in Russian).
28. Korinevsky N.A., Levitsky R.R. // Teor. i Matem. Fiz., 1980, vol. 42, No. 3, p. 416–429 (in Russian).
29. Levitsky R.R., Korinevsky N.A., Stasyuk I.V. // Phys. Stat. Sol. (b), 1978, vol. 88, No. 1, p. 51–63.
30. Strukov B.A., Amin M., Kopcik V.A. // Phys. Stat. Sol., 1968, vol. 27, p. 741–749.
31. Strukov B.A., Baddur A., Zinenko V.N., Mishchenko A.V., Kopcik V.A. // Fiz. Tverd. Tela, 1973, vol. 15, No. 5, p. 1388–1394 (in Russian).
32. Stephenson C.C., Corbella J.M., Russell L.A. // J. Chem. Phys., vol. 21, No. 6, p. 1110.
33. Fairall C.W., Reese W. // Phys. Rev. B, 1974, vol. 10, No. 3, p. 882–885.
34. Strukov B.A., Baddur A., Kopcik V.A., Velichko I.A. // Fiz. Tverd. Tela, 1972, vol. 14,

No. 4, p. 1034–1039 (in Russian).
35. Shuvalov L.A., Zheludev I.S., Mnatzakanyan A.V., Ludupov Ts.-Zh., Fiala I. // Bull. Ac. Sci. USSR, Ser. phys., 1967, vol. 31, No. 11, p. 1919–1922 (in Russian).
36. Fairall C.W., Reese W. // Phys. Rev. B, 1972, vol. 6, No. 1, p. 193–199.
37. Samara G.A. // Ferroelectrics, 1973, vol. 5, p. 25–37.
38. Fairall C.W., Reese W. // Phys. Rev. B, 1973, vol. 8, No. 7, p. 3475–3478.
39. Zolototrubov Yu.S., Strukov B.A., Taraskin S.A., Kamysheva L.N. // Bull. Ac. Sci. USSR, Ser. phys., 1975, vol. 39, No. 4, p. 782–786 (in Russian).
40. Meriakri V.V., Poplavko Yu.M., Ushatkin E.F. // Zhurn. Techn. Fiz., 1974, vol. 44, No. 5, p. 1111–1113 (in Russian).
41. Amin M., Strukov B.A. // Fiz. Tverd. Tela, 1968, vol. 10, No. 10, p. 3158–3160 (in Russian).
42. Blinc R., Burgar M., Levstik A. // Sol. St. Commun., 1973, vol. 12, No. 6, p. 573–576.
43. Strukov B.A., Korzhuev M.A., Baddur A., Kopcik V.A. // Fiz. Tverd. Tela, 1971, vol. 13, No. 7, p. 1872–1877 (in Russian).
44. Sidnenko Ye.V., Gladkii V.V. // Kristallografia, 1973, vol. 18, No. 1, p. 138–142 (in Russian).
45. Sugie H., Okada K., Kanno K. // J. Phys. Soc. Japan, 1971, vol. 33, No. 4, p. 1727–1731.
46. Magataev V.K., Gladkii V.V., Zheludev I.S. // Bull. Ac. Sci. USSR, Ser. phys., 1975, vol. 39, No. 4, p. 778–781 (in Russian).
47. Eberhard J.W., Horn P.M. // Solid State Commun., 1975, vol. 16, No. 12, p. 1343–1345.
48. Gladkii V.V., Sidnenko Ye.V. // Fiz. Tverd. Tela, 1971, vol. 13, No. 6, p. 1642–1648 (in Russian).
49. Benepe J.W., Reese W. // Phys. Rev. B, 1971, vol. 3, No. 9, p. 3032–3039.
50. Azoulay J., Grinberg Y., Pelah I., Wiener E. // J. Phys. Chem. Solids, 1968, vol. 29, No. 5, p. 843–849.
51. Reese W. // Phys. Rev., 1969, vol. 181, No. 2, p. 905–919.
52. Reese W., May L.F. // Phys. Rev., 1967, vol. 162, No. 2, p. 510–518.
53. Garber S.R., Smolenko L.A. // Zhurn. Eksper. i Theor. Fiz., 1973, vol. 64, No. 1, p. 181–194 (in Russian).
54. Malek Z., Shuvalov L.A., Fiala I., Strajblova Ja. // Kristallografia, 1968, vol. 13, No. 5, p. 825–830 (in Russian).
55. Kryzhanovskaya N.A., Dovchenko G.V., Dudnik E.F., Mishchenko A.V. // Bull. Ac. Sci. USSR, Ser. phys., 1975, vol. 39, No. 5, p. 1031–1035 (in Russian).
56. Smolneskii G.A. Physics of Ferroelectric Phenomena. Leningrad, Nauka, 1985 (in Russian).
57. Kennedy N.S.J., Nelmes R.J. // J. Phys. C: Solid St. Phys., 1980, vol. 13, No. 26, p. 4841–4853.
58. Nelmes R.J., Meyer G.M., Tibballs J.E. // J. Phys. C: Solid St. Phys., 1982, vol. 15, No. 1, p. 59–75.
59. William R., Cook, Jr. // J. Appl. Phys., 1967, vol. 38, No. 4, p. 1637–1642.
60. Wiseman G.G. // JEE Transactions on Electron Devices, 1969, vol. ED–16, No. 6, p. 588–593.
61. Motedi H., Kuramoto K., Nakamura E. // J. Phys. Soc. Japan, 1983, vol. 52, No. 4, p. 1131–1133.

62. Deguchi K., Nakamura E. // J. Phys. Soc. Japan, 1980, vol. 49, No. 5, p. 1887–1891.
63. Vasiljevskaja A.S., Sonin A.S. // Fiz. Tverd. Tela, 1971, vol. 13, No. 6, p. 1550–1556 (in Russian).
64. Mayer R.J., Bjorkstam J.L. // J. Phys. Chem. Solids, 1962, vol. 23, p. 619–620.
65. Pereverzeva L.P., Poplavko Yu.M., Petrov V.M., Makarevskaya E.V., Rez I.S. // Kristallografia, 1973, vol. 18, No. 3, p. 645–646 (in Russian).
66. Pereverzeva L.P. // Bull. Ac. Sci. USSR, Ser. phys., 1971, vol. 35, No. 12, p. 2613–2614 (in Russian).
67. Volkova Je. N. Doctoral thesis, Moscow, 1991 (in Russian).
68. Levitskii R.R., Sorokov S.I., Baran O.R., Pyndzyn I.M. // J. Phys. Studies, 1998, vol. 2, No. 3, p. 391–400 (in Ukrainian).
69. Levitskii R.R., Lisnii B.M., Baran O.R. Preprint of the Institute for Condensed Matter Physics, ICMP–01–10U, Lviv, 2001, 43 p. (in Ukrainian).
70. Stasyuk I.V., Levitskii R.R., Moina A.P. // Phys. Rev. B, 1999, vol. 59, No. 13, p. 8530–8540.
71. Stasyuk I.V., Levitskii R.R., Zachek I.R., Moina A.P. // Phys. Rev. B, 2000, vol. 62, No. 10, p. 6198–6207.
72. Levitskii R.R., Moina A.P., Lisnii B.M. Preprint of the Institute for Condensed Matter Physics, ICMP–00–12U, Lviv, 2000, 36p. (in Ukrainian).

Термодинаміка та діелектричні властивості сегнетоелектриків KH_2PO_4, RbH_2PO_4, KH_2AsO_4, RbH_2AsO_4

Р.Р.Левицький, Б.М.Лісний, О.Р.Баран

Інститут фізики конденсованих систем НАН України,
79011 Львів, вул. Свєнціцького, 1

Отримано 28 травня 2001 р.

В рамках моделі протонного впорядкування з врахуванням короткосяжних і далекосяжних взаємодій та тунелювання протонів на водневих зв'язках досліджуються в наближенні чотиричастинкового кластера термодинамічні та статичні діелектричні властивості сегнетоелектриків типу KH_2PO_4. Проведено кількісне порівняння результатів теоретичного розрахунку з відповідними експериментальними даними та з результатами розрахунків інших авторів. Показано, що при належному виборі параметрів теорії має місце дуже добрий кількісний опис наявних експериментальних даних для температурних залежностей спонтанної поляризації, теплоємності, поздовжньої і поперечної статичних діелектричних проникностей, а також для температури та константи Кюрі-Вейса.
Обговорюється придатність моделі до опису кристалів KH_2PO_4, RbH_2PO_4, KH_2AsO_4, RbH_2AsO_4 без врахування стрикції, флуктуацій та інших ефектів.

Ключові слова: *кластерне наближення, KDP, тунелювання, фазовий перехід, діелектрична сприйнятливість, температура Кюрі-Вейса, константа Кюрі-Вейса*

PACS: *77.22.Ch, 77.80.Bh, 77.84.Fa*